OPTIMUM CONTROL STRATEGIES FOR SOLAR HEATING AND COOLING SYSTEMS

A THESIS

Presented to

The Faculty of the Division of Graduate Studies

By

Henry Jung

In Partial Fulfillment

of the Requirements for the Degree

Master of Science in Mechanical Engineering

Georgia Institute of Technology

August, 1977

OPTIMUM CONTROL STRATEGIES FOR SOLAR

HEATING AND COOLING SYSTEMS

Approved:

R. R. Williams, Chairman

S. V. Hanagud

J. M. Mills

Date approved by Chairman August 1, 1977

ACKNOWLEDGMENTS

I am deeply grateful to my thesis advisor, Dr. J. R. Williams, and to the members of my reading committee, Dr. S. V. Hanagud and Dr. J. M. Mills.

Special thanks are due to members of the Solar Energy Laboratory of the School of Mechanical Engineering at Georgia Institute of Technology.

Funds provided by the Canadian National Research Council for making graduate studies possible are acknowledged.

I am deeply indebted to my wife, Cecilia, for her patience, tolerance, understanding, and the sacrifices that she made during the years of my graduate study.

In addition, I wish to thank my typist, Ms. Shirleye McCombs, for her enthusiasm, co-operation, and promptness in typing this thesis.

TABLE OF CONTENTS

Page

ACKNOWLEDGMENTS ii

LIST OF TABLES v

LIST OF ILLUSTRATIONS vi

NOMENCLATURE viii

SUMMARY xiii

Chapter

I. INTRODUCTION 1

General
Purpose of This Research
Literature Survey

II. SOLAR SYSTEM 4

Description
Control Modes

III. COMPONENT MODELS 12

Solar Collector
Building
Fan-Coil Unit
Thermal Storage Tanks
Absorption Chiller

IV. SOLAR RADIATION AND WEATHER DATA 25

Solar Radiation
Specific Humidity of Air

V. COMPUTER SIMULATION 34

Program Description
Method of Integration
System Parameters

TABLE OF CONTENTS (Continued)

		Page
VI.	DISCUSSION OF RESULTS	53
	Program Evaluation Parametric Studies System Simulation	
VII.	CONCLUSIONS AND RECOMMENDATIONS	78
	Conclusions Recommendations	
APPENDICES		80
A.	THERMAL CAPACITANCE CALCULATIONS OF ISOTHERMAL SECTIONS	81
B.	FAN-COIL PERFORMANCE DATA, DERIVATION OF THE SENSIBLE TO TOTAL HEAT TRANSFER RATIO, R_Q	87
C.	ABSORPTION CHILLER PERFORMANCE DATA	91
D.	METEOROLOGICAL DATA FOR EIGHT SELECTED DAYS IN 1964 FOR ATLANTA	93
BIBLIOGRAPHY	. . . . .	102

LIST OF TABLES

Table		Page
1.	Experimental Ratio of Hourly Total Radiation to Daily Total Radiation	30
2.	System Parameters	50
3.	Fan-Coil Performance Data	88
4.	Absorption Chiller Performance Data	92
5.	Meteorological Data for Eight Selected Days	94

LIST OF ILLUSTRATIONS

Figure		Page
1.	Schematic of Multi-Mode Solar System	5
2.	Classroom Lay-out	7
3.	Logic Diagrams: Heating	10
4.	Logic Diagrams: Cooling	11
5.	Thermal Analogy of a Wall	15
6.	Ratio of Daily Diffuse Radiation to Daily Total Radiation	27
7.	Experimental Ratio of Hourly Total Radiation to Daily Total Radiation	29
8.	Flow Charts:	
	a. Flow Chart of Atm	37
	b. Flow Chart of Chill	38
	c. Flow Chart of Coil	39
	d. Flow Chart of Col	40
	e. Flow Chart of Contr	41
	f. Flow Chart of Load	42
	g. Flow Chart of Main	43
	h. Flow Chart of Moist	44
	i. Flow Chart of Stor	45
	j. Flow Chart of Wethr	46
9.	Mode Selection: Heating	47
10.	Mode Selection: Cooling	48
11.	Example of Computer Results for Heating Operation:	
	a. Temperature Profiles	55
	b. Heat Transfer Rates	56
	c. Mode of Operation	57
12.	Example of Computer Results for Cooling Operation:	

LIST OF ILLUSTRATIONS (Continued)

Figure		Page
	a. Temperature Profiles	58
	b. Heat Transfer Rates	59
	c. Mode of Operation	60
13.	Effect of Hot Storage Capacity on Collector Efficiency: Heating	62
14.	Effects of Hot Storage Capacity: Cooling	63
15.	Effect of Collector Area on Collector Efficiency: Heating	64
16.	Effects of Collector Area: Cooling	65
17.	Effect of Collector Fluid Flow Rate on Collector Efficiency: Heating	67
18.	Effect of Increasing Hot Water Flow Rate on Chilled Water Production: Cooling	68
19.	Effect of Collector Loss Coefficient on Collector Efficiency: Heating	69
20.	Effect of Collector Loss Coefficient on Collector Efficiency: Cooling	70
21.	Effect of Differential Control Temperature Between Collector and Hot Storage on Collector Efficiency: Heating	71
22.	Effects of Differential Control Temperature Between Collector and Hot Storage: Cooling	72
23.	System Performance for January 1964	75
24.	System Performance for June 1964	76
25.	Effects of Changing Collector Slope: Cooling	77

NOMENCLATURE

Symbol		Unit
A	area	m^2
AF	allowance factor for light fittings	dimensionless
B_a	barometric pressure	$in(H_g)$
C_A	lumped value of collector capacitance	$J/m^2\ ^oC$
C	thermal conductance	$W/m^2\ ^oC$
C_{air}	capacitance of air, density x specific heat	$J/m^3\ ^oC$
Cap	fraction of design delivered chilled water capacity	dimensionless
Cop	coefficient of performance	dimensionless
C_p	specific heat of water	J/kg^oC
E_c	water equivalent of fan-coil cold stream, mass rate x specific heat	J/s^oC
E_h	water equivalent of fan-coil hot stream, mass rate x specific heat	J/s^oC
f	surface conductance	$W/m^2\ ^oC$
F'	collector efficiency factor	dimensionless
F_R	collector heat removal factor	dimensionless
G	rate of addition or removal of moisture	kg/s
H	total solar radiation incident on a horizontal surface	W/m^2
ha	enthalpy of air	kJ/kg of dry air
K_D	ratio of daily diffuse radiation on a horizontal surface to daily total	

NOMENCLATURE (Continued)

Symbol		Unit
	radiation on a horizontal surface	dimensionless
K_T	ratio of daily total radiation on a horizontal surface to extraterrestrial daily insolation on a horizontal surface	dimensionless
m	mass flow rate	kg/s
M_A	mass of air in classroom interior	kg
$M_i C_i$	effective thermal capacitance of the interior	$J/^oC$
$M_w C_w$	effective thermal capacitance of the isothermal section	$J/m^2\ ^oC$
M_S	mass of thermal storage	kg
n	the day of the year	dimensionless
P_d	saturated steam pressure at air dry-bulb temperature	$in(H_g)$
P_S	partial pressure of the water vapour in air	$in(H_g)$
Q	rate of heat transfer	W
Qu	rate of useful solar energy gain	W
R	ratio of total radiation on a tilted surface to that on a horizontal surface	dimensionless
R_b	ratio of beam radiation on a titled surface to that on a horizontal surface	dimensionless
R_C	rate of air volume changes	s^{-1}
r_d	ratio of hourly diffuse to daily diffuse radiation	dimensionless
RH	relative humidity of air	dimensionless
R_Q	ratio of sensible to total heat trans-	

NOMENCLATURE (Continued)

Symbol		Unit
	fer defined by Eq. (3.15)	dimensionless
r_T	ratio of hourly total to daily total radiation	dimensionless
S	specific humidity of air, kg of water vapour per kg of air	dimensionless
s	slope of surface from the horizontal	degrees
Sc	shade factor of windows	dimensionless
T	temperature	^oC
t	time	s
U	overall heat transfer coefficient	$W/m^2\ ^oC$
UF	use factor of light fittings	dimensionless
U_L	overall loss coefficient of flat-plate collector	$W/m^2\ ^oC$
V_R	volume of classroom interior	m^3
w	wind speed	m/s
W	total rated light wattage of all fittings	W
W_s	mass flow rate to or from the storage tank	kg/s

Greek Letter Symbols

α	absorptance of solar radiation	dimensionless
γ	surface azimuth angle	degrees
δ	declination	degrees
η	ground reflectance	dimensionless
θ_T	angle between incident beam radiation and normal to the surface	degrees

NOMENCLATURE (Continued)

Greek Letter Symbols		Unit
θ_z	angle between incident beam radiation and vertical	degrees
ρ	density of air	kg/m^3
τ	transmittance of solar radiation	dimensionless
ϕ	latitude	degrees
ω	hour angle	degrees
ω_s	sunset hour angle	radians

Subscripts

amb	ambient
aux	auxiliary
b	beam radiation
c	collector
ci	cold inlet fan-coil stream
co	cold outlet fan-coil stream
cl	fan-coil
d	diffuse radiation, door, dry-bulb
DD	daily diffuse
DE	daily extraterrestrial
d_i	inlet dry-bulb
do	outlet dry-bulb
DT	daily total
f	floor
hi	hot inlet fan-coil stream
ho	hot outlet fan-coil stream

NOMENCLATURE (Continued)

Subscripts

i	interior, infiltration, inlet
ℓ	loss to surroundings
m	mean collector fluid
o	exterior, outlet
p	people
r	roof
rad	solar radiation
S	storage, sensible heat
T	total radiation, total heat removed
twd	all classroom windows
w	isothermal section, wall, wet-bulb
we	east wall
wd	window
wn	north wall
ws	south wall
ww	west wall

Superscript

z	zero-capacitance model

SUMMARY

A Computer program has been developed for simulating the dynamic thermal behavior of a multi-mode solar heating and cooling system, currently being installed at Georgia Tech. This system has the capability of operating in 12 different experimental modes: four for space heating and eight for chilled water cooling. Because the system is inherently transient, the mathematical model of the system includes the effects of thermal capacitance of the flat-plate collectors and the building structure on system response and performance.

Parametric studies were carried out to determine the effects on system performance of several control and component parameters, including thermal storage capacity, flow rates, collector area, and differential control temperature between the collector and hot storage. Meteorological data representing extreme combinations of sky cover condition and ambient air temperature of eight selected days in 1964 for Atlanta were used in these studies.

The outcome of this study is a comprehensive set of control strategies that would optimize the performance of this particular multi-mode solar heating and cooling system.

CHAPTER I

INTRODUCTION

General

The Solar Energy Laboratory in the School of Mechanical Engineering at Georgia Institute of Technology has designed, and is currently installing an experimental solar energy system to provide space heating and chilled water cooling for a 122 m^2 classroom. It is the first such project at Georgia Tech to integrate solar powered air conditioning and space heating.

An outstanding feature of this system is its versatility to operate in 12 different experimental modes: four for space heating and eight for chilled water cooling. Each mode provides a different method of solar heat transfer and employs a particular arrangement of system components, i.e., system components are to be interconnected in a specific manner. The selection of a particular mode of operation is based on several factors which include load demand, solar energy availability, weather conditions, and the temperatures of the cold and hot thermal storages at that instant of time.

Mathematical simulation using a digital computer is a powerful tool for the analysis of solar system performance. This tool is particularly effective for the analysis of the dynamic thermal behavior of an inherently transient system with an immense complexity of component interdependencies.

Purpose of This Research

The objective of this thesis is to develop a comprehensive mathematical model which will determine the effects of several control and component parameters on the performance of a multi-mode solar heating and cooling system, so control strategies could be developed for the solar system to operate in an optimized or near-optimized manner.

Literature Survey

A very limited number of published papers are currently available in the areas of optimization, operation, and computer simulation of multi-mode solar heating and cooling systems.

Ward, et al. (22) presented a paper on the comparative performance of four different modes of operation for the solar heating and cooling system at Colorado State University Solar House I. They concluded that the subsystem alterations, or modes of operation improve the efficiency of the solar system but come at an added cost in terms of installation and maintenance.

Wahlig and co-workers (21) at Lawrence Berkeley Laboratory of the University of California are currently developing and testing an electronic control system capable of operating a solar system with 26 different modes. The heart of the controller circuit consists of one or more Programmable Read-Only Memory (PROM) modules, containing an operating algorithm which defines modes of operation based on system temperature measurements.

The application of optimization techniques to solar heating and

cooling systems has been carried out by Anderson and Rauch (1). They used optimization techniques to determine values for the control variables, i.e., flow rates for all flow paths that will maximize a payoff function subject to the constraints on the controls. The payoff function represents a net solar energy gain minus an equivalent cost of human discomfort when the room temperature is not held at its desired value.

Most of the efforts undertaken in computer simulations have been concerned with the prediction of thermal performance of a conventional solar system for providing residential heating, cooling, and service hot water. A number of papers on such studies have been published by the Solar Energy Laboratory at the University of Wisconsin (12, 17). Very little, as revealed by the literature survey, is being done on computer simulations of multi-mode solar heating and cooling systems.

CHAPTER II

SOLAR SYSTEM

Description

The experimental solar heating and cooling system is shown schematically in Figure 1. The energy transfer and storage medium is water, except for a separate and self-contained loop with 12 aluminum collectors which uses water and ethylene-glycol solution as a preventive measure for freeze protection.

The system is presently being installed in the Space Science and Technology building at Georgia Tech. The collector array and chiller are located on the roof, and the thermal storage tanks are placed next to the building at ground level. The system is piped to a classroom in the Mechanical Engineering building adjacent to the S.S.T. building.

The collector array consists of 46 flat-plate solar collectors with a total area of 74.3 m^2. The collectors, produced by four different manufacturers, are both single and double-glazed and utilize a variety of absorber coatings. They are mounted in two parallel rows facing south. The tilt angle is set at 45^o from the horizontal.

Two unpressurized steel tanks, each has 7.3 m^3 capacity, are used to store hot and chilled water. The tanks are insulated with 0.051 m of polyurethane and 0.152 m of polystyrene. They are elevated above the ground on a 0.038 m-thick wooden platform covered with two layers of roofing material, 0.051 m of foam glass and 0.064 m of polystyrene.

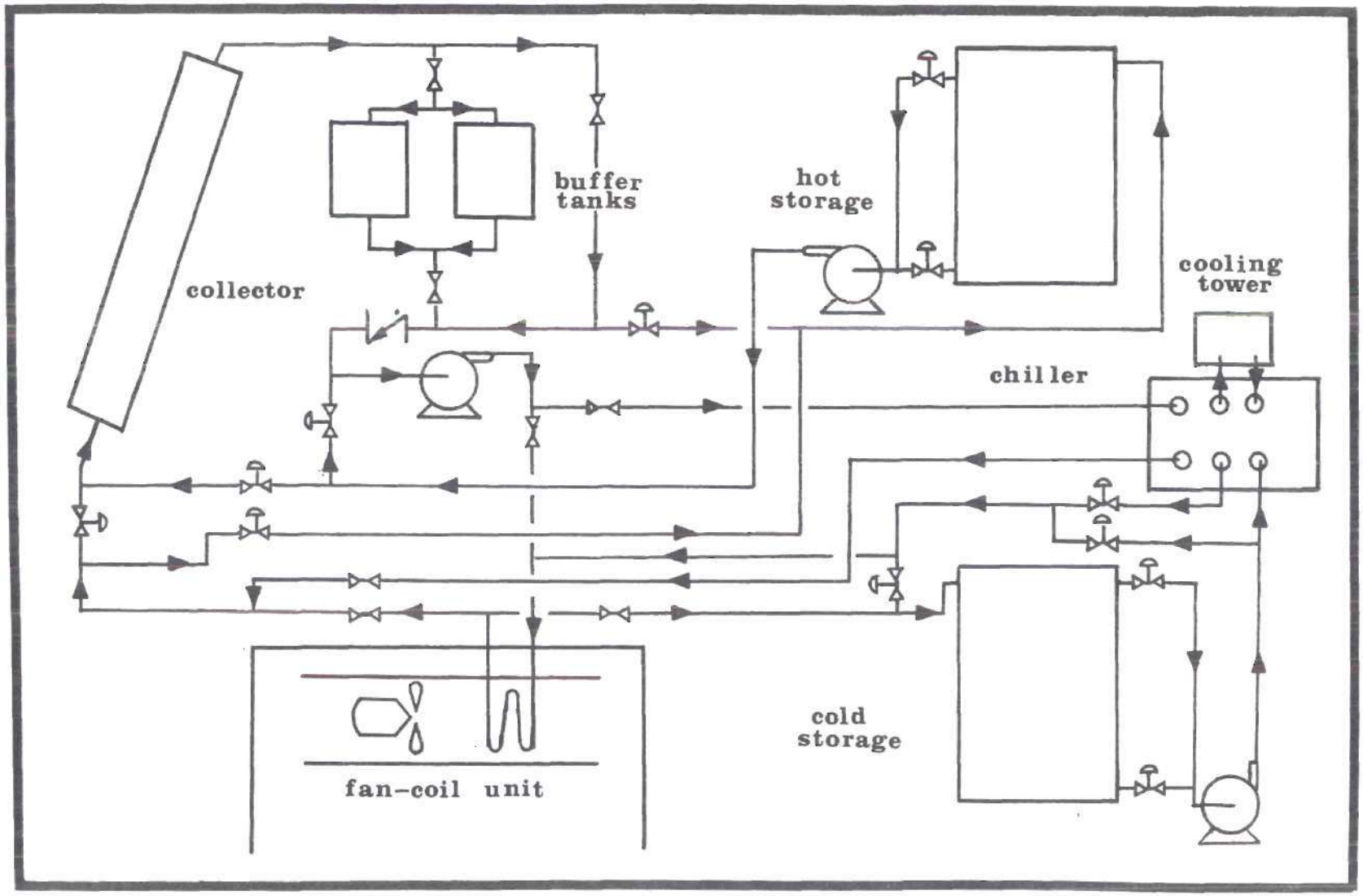

Figure 1. Schematic of Multi-Mode Solar System

The classroom to be heated and cooled has a floor area of 122 m^2. As shown in Figure 2, it has three exterior walls. The window areas of the south and west walls are 35% and 40% of each total wall area, respectively.

The system uses a 10.5 kW lithium bromide absorption chiller to provide chilled water. Condensing water supplied by a cooling tower is used to remove the waste heat of the chiller.

A 11.5 kW fan-coil unit is used to transfer heat between the system and the classroom. Flows through the system are regulated by pumps, on-off solenoid valves, and associated piping.

Control Modes

Logic diagrams for the 12 solar system configurations containing all practical heat transfer paths between components are shown in Figures 3 and 4. Criteria governing each mode of operation are also given. The components are represented by the following symbols: collector (C), hot storage tank (THS), cold storage tank (TCS), fan-coil unit (CL), chiller (CH), and the classroom to be heated and cooled (BLG).

These 12 solar system configurations were selected because they represent the most effective scheme of collecting and utilizing solar energy for all weather conditions encountered.

For heating operation, four different modes of operation are utilized. When both solar energy gain and load demand exist, mode 1 is used. In this mode of operation, water is circulated from the hot storage tank to the collectors, then to the fan-coil unit, and finally back to the storage tank. The water from the hot storage tank picks up heat

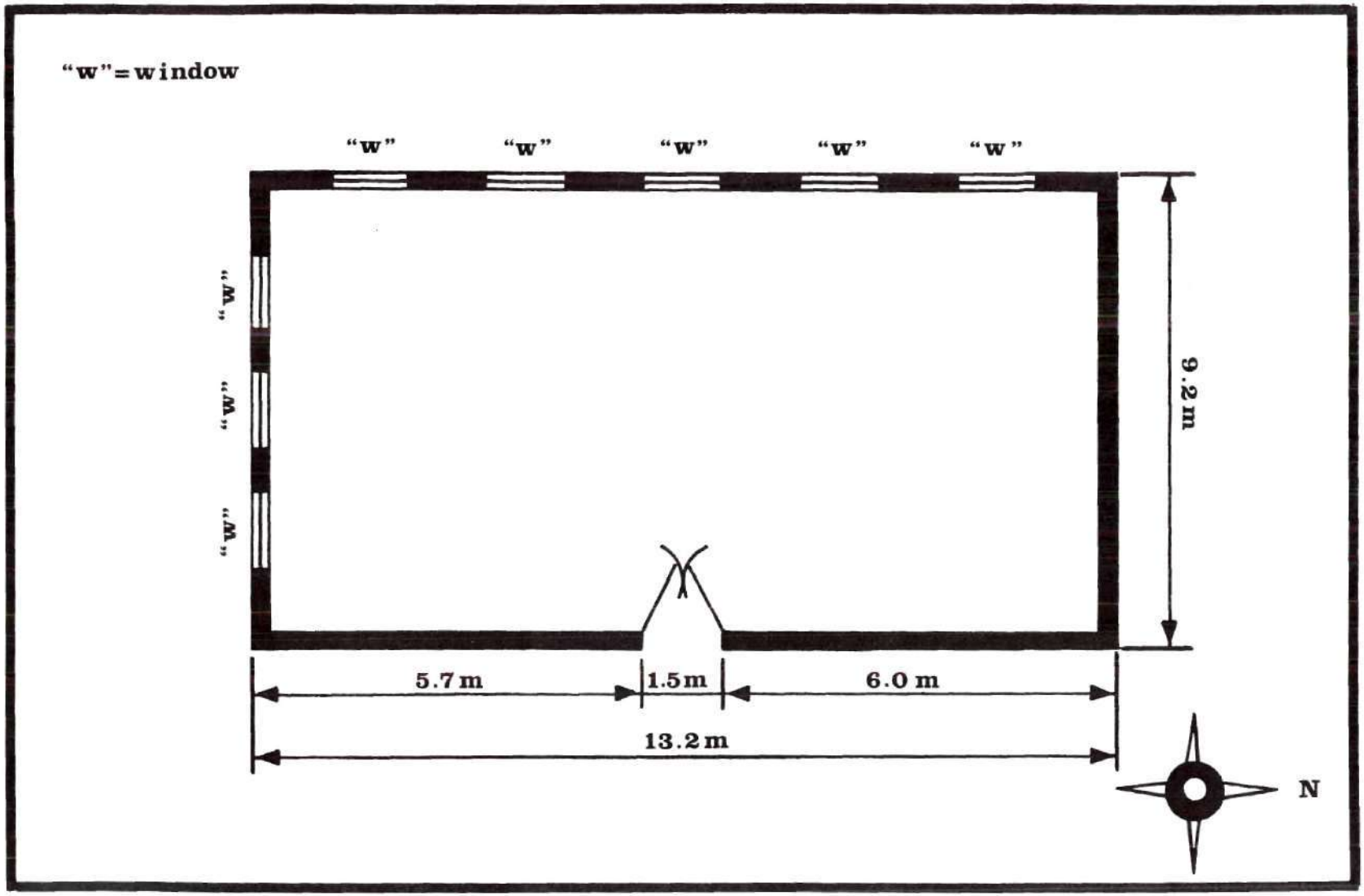

Figure 2. Classroom Lay-out

when it passes through the collector array and releases this heat to the classroom interior by means of heat exchange in the fan-coil unit. If only solar energy gain exists, mode 2 is used to collect and store this heat. When solar energy is not available, heating load demand is met by using the energy stored in the hot storage tank to heat up the classroom as depicted by mode 3. For weather condition with low solar radiation intensity and high ambient air temperature, both solar energy gain and load demand do not exist. In this case the system is shut down and all flows are turned off.

There are eight modes of operation for cooling. In modes 1, 2, 3, and 4 the absorption chiller is in operation because the inlet hot water temperature is greater than 76.7^{o}C, required for efficient operation of the chiller. In modes 1 and 3, the available solar energy is used to increase the temperature of the circulating fluid from the hot storage tank to 76.7^{o}C required by the chiller unit. On the other hand, in modes 2 and 4 solar energy is not available for heating the circulating fluid, but the water temperature in the hot storage tank is sufficient to meet the 76.7^{o}C requirement of the chiller. The chilled water produced in all these modes of operation could be used to cool the classroom, if cooling load demand exists as in cases for modes 3 and 4, or stored in the chilled water storage tank for future use as in cases for modes 1 and 2.

When the 76.7^{o}C requirement of the chiller can not be met, the chiller is shut down. The circuits for collecting solar energy and for cooling the classroom interior are then operated individually or separately together. These are the cases for modes 5, 6, and 8.

As in heating operation, when there are no solar energy gain and load demand, and the water temperature of the hot storage tank is insufficient to drive the chiller, the system is shut down and all flows are turned off. This is the case for mode 7.

The physical operation of each energy flow configuration is accomplished by the opening and closing of valves, and turning on and off of pumps.

The criteria governing each mode of operation are based on selected temperature measurements. For heating operation, three temperature measurements are needed: the differential temperature between the collector outlet and the hot storage, the temperature of the collector plate, and the temperature of the classroom.

When the temperature of the collector outlet is greater than the hot storage temperature by a prescribed value, flow from the hot storage tank to the collector is initiated. The flow is turned off when the temperature difference drops below a set point. As a protective measure, the flow to the collector is turned off whenever the collector outlet temperature exceeds $100^{o}C$ to prevent boiling of the heat transfer medium, water. Similarly, the flow to the heating coil is initiated whenever a load demand exists, i.e., when the temperature of the classroom drops below a desired value. When all flows are off, the system automatically drains down for freeze protection.

For cooling operation, an additional temperature measurement is required for the efficient operation of the chiller. Flows to the chiller are turned off whenever the hot water inlet temperature to the generator drops below $76.7^{o}C$, since lower temperatures are not acceptable.

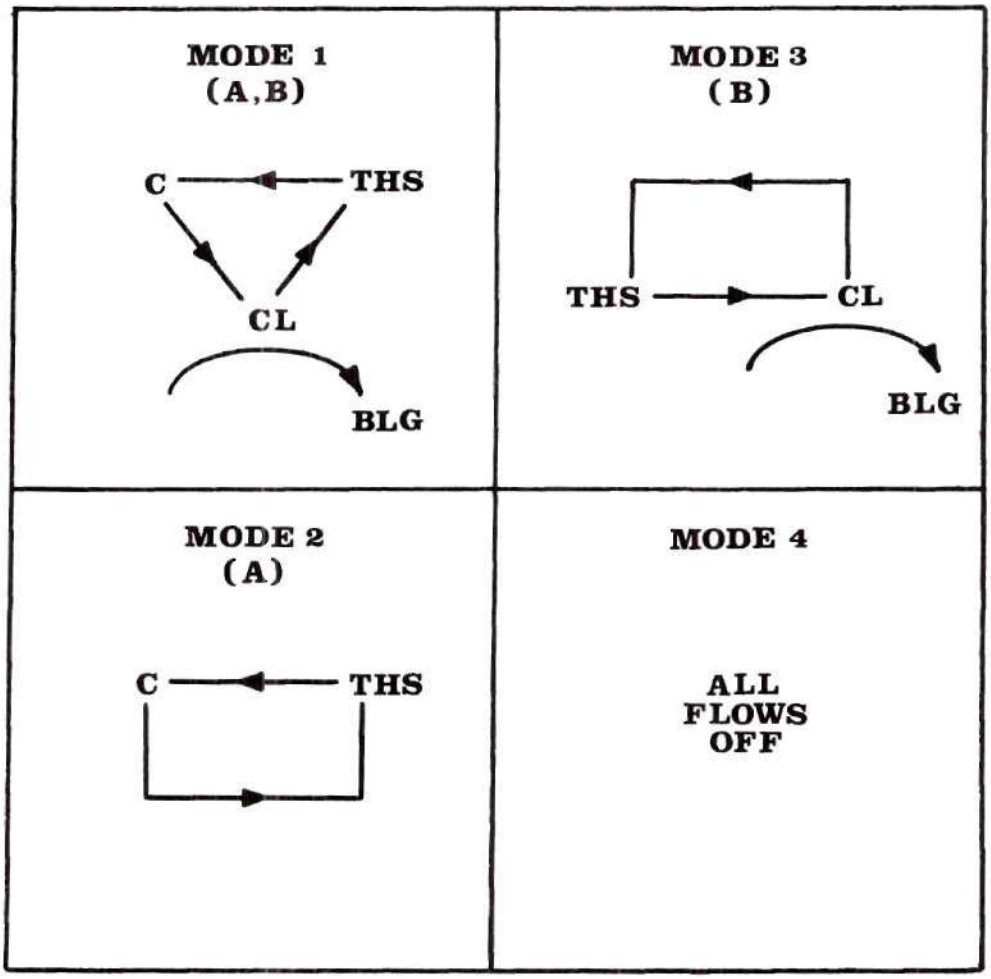

Criteria for operation:

A. solar energy gain
B. load demand

Figure 3. Logic Diagrams: Heating

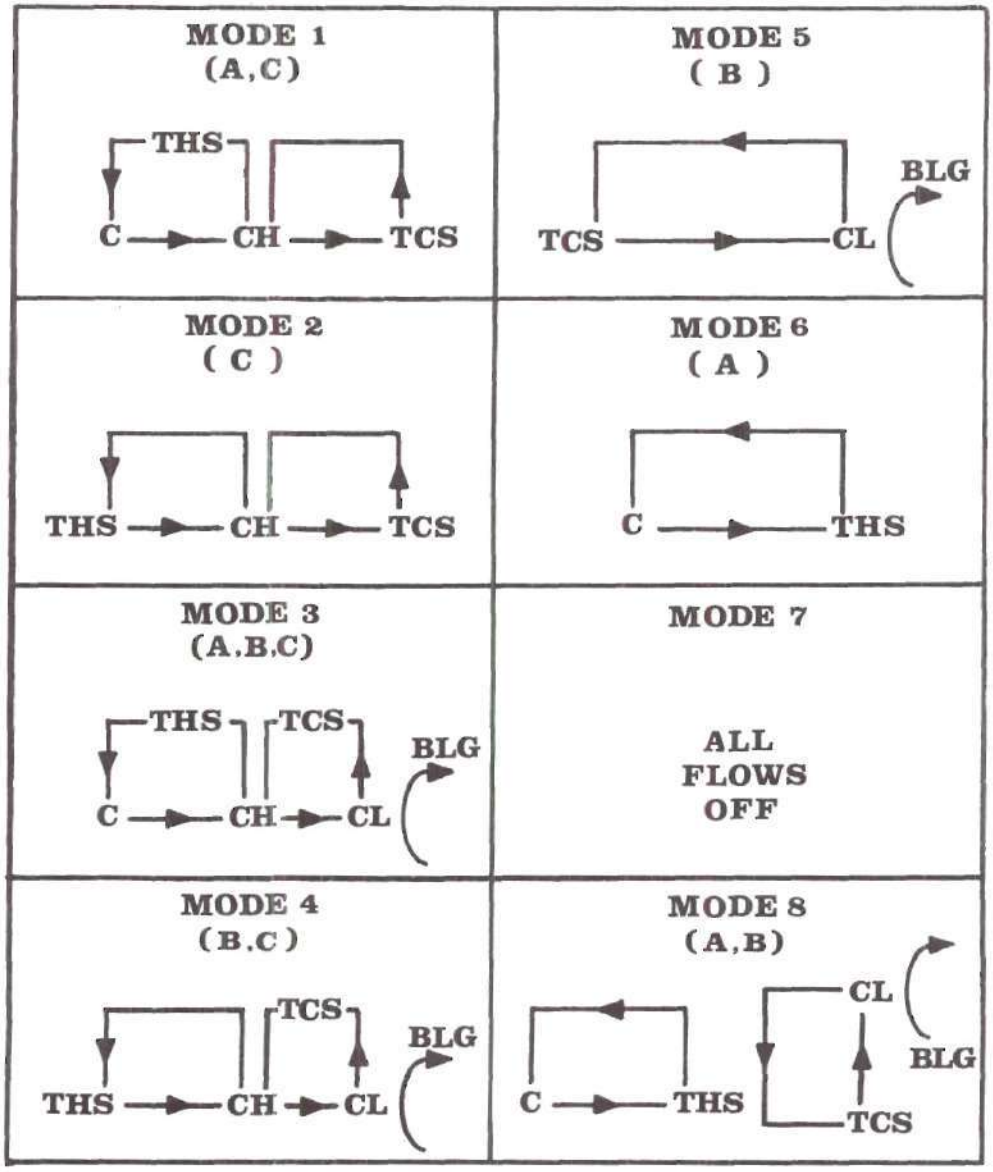

Criteria for operation:

A. solar energy gain
B. load demand
C. inlet chiller hot-water temperature greater than 76.7°C

Figure 4. Logic Diagrams: Cooling

CHAPTER III

COMPONENT MODELS

Solar Collector

The operation of a multi-mode solar collector system is inherently transient. The collectors are exposed to continuously variable weather conditions. The flow to the collector array is turned on or off depending on the mode of operation at that instant of time. For this system there is no such thing as steady-state operation.

The zero-capacitance models of Hottel and Woertz (9), Hottel and Whillier (8) which assume the collector to be in equilibrium with its environment at any instant of time could not be used to model the actual behavior of a transient system. A better model is the one-node capacitance model developed by Klein, et al. (13) which accounts for the capacitance effects of the solar collector. The model assumes that the collector capacitance can be lumped with the collector mean fluid temperature. The governing differential equation which includes the effect of pump control on the mean collector fluid temperature is

$$C_A \frac{dT_m}{dt} = (1 - \gamma)\left[HR(\tau\alpha) - U_L(T_m - T_{amb})\right]$$

$$+ \gamma\left\{F'\left[HR(\tau\alpha) - U_L(T_m - T_{amb})\right]\right.$$

$$\left. - F_R\left[HR(\tau\alpha) - U_L(T_{in} - T_{amb})\right]\right.$$

$$- \frac{2m_c C_p}{A_c} (T_m - T_m^z) \Big\} \qquad (3.1)$$

where

C_A = lumped value of collector capacitance

dT_m/dt = time rate of change of the mean fluid temperature

γ = 0 if the pump is off and 1 if the pump is on

H = total solar radiation (beam + diffuse) incident on a horizontal surface

R = ratio of total radiation on a tilted surface to that on a horizontal surface

$\tau\alpha$ = cover transmittance times plate absorptance

U_L = collector overall loss coefficient

T_m = mean collector fluid temperature

T_{amb} = ambient air temperature

F' = collector efficiency factor

F_R = collector heat removal factor

T_{in} = inlet fluid temperature

m_c = mass flow rate of fluid through the collector

C_p = specific heat of collector fluid

A_c = area of collector

T_m^z = mean fluid temperature computed by the zero-capacitance model

$$= T_{in} + \frac{F_R}{U_L} \left[HR(\tau\alpha) - U_L(T_{in} - T_{amb}) \right] \left[\frac{1}{F_R} - \frac{1}{F'} \right]$$

The fluid exit temperature, T_{out}, is assumed to be equal to

$$T_{out} = T_{out}^z + 2\left[T_m - T_m^z \right] \qquad (3.2)$$

where T_{out}^{z} = exit fluid temperature computed by the zero-capacitance model

$$= T_{in} + \frac{F_R A_c}{\dot{m}_c C_p}\left[HR(\tau\alpha) - U_L(T_{in} - T_{amb})\right]$$

The total useful energy gain of the collector is given by

$$Qu = \dot{m}_c C_p (T_{out} - T_{in}) \qquad (3.3)$$

Building

The classroom is modeled as a box-like structure. Exterior walls and roof are treated as isothermal sections. For the walls, treating them as isothermal sections is a good approximation. The effective thermal capacitance of each wall is sufficiently large to cause the rate of temperature change to be small; consequently, each wall could be approximated as an isothermal section. For the roof, however, the isothermal approximation is not adequate. The roof is composed of several structural and insulating materials, and modeling the roof as an isothermal section would be a conservative representation of the actual system. The need to minimize computer time and cost, and the lack of structural information of the classroom justify this simple modeling approach.

The effective thermal capacitance of each section is the sum total of thermal capacitances for all the materials present. A detailed calculation of the thermal capacitance for each section is presented in Appendix A. An example of a cross section of a wall and its equivalent thermal analogue is illustrated in Figure 5. The node of the isothermal

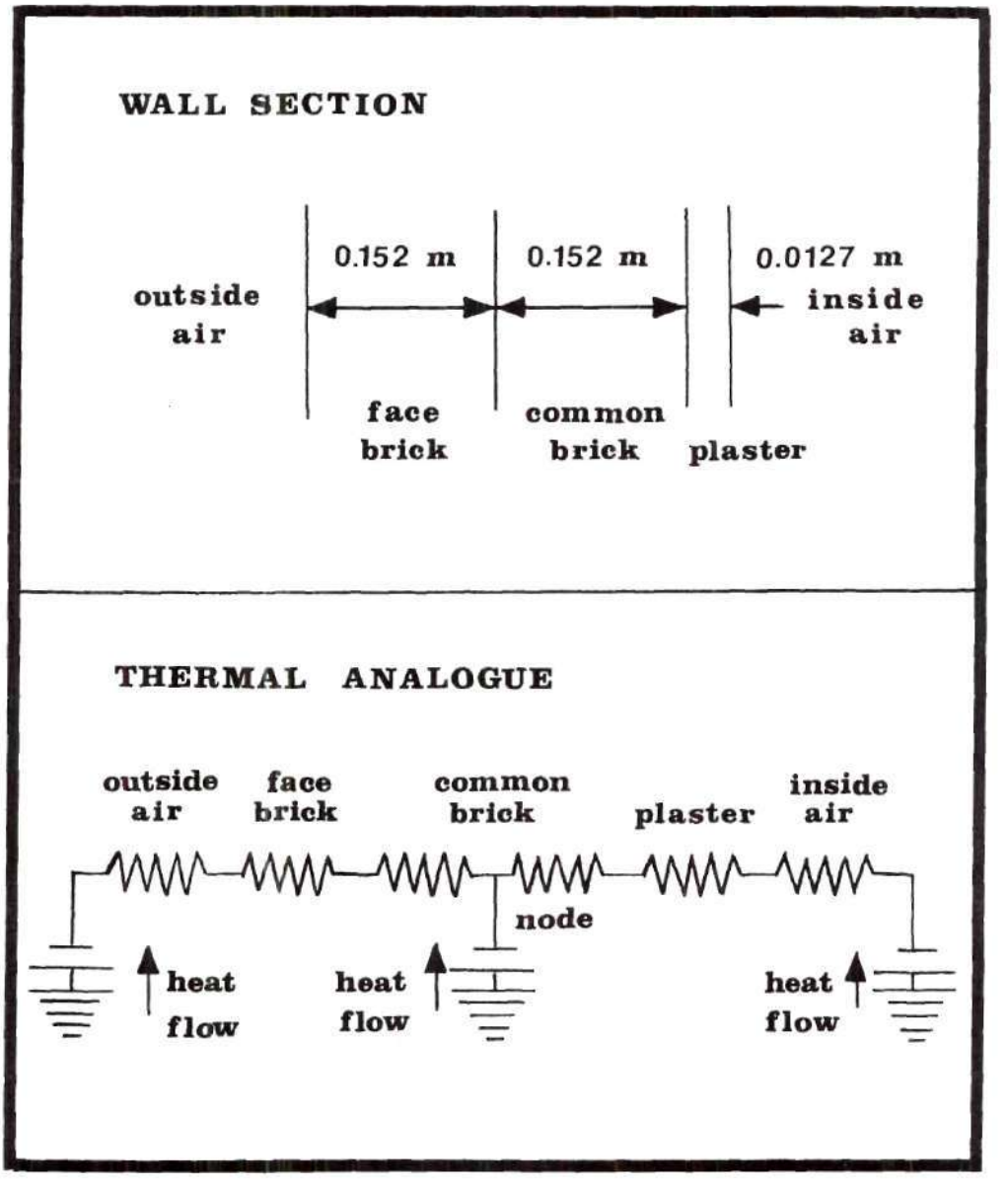

Figure 5. Thermal Analogy of a Wall

section is assumed to be at a point in the wall where the resistances to the interior and exterior are approximately equal. The energy rate equation for each isothermal section can be expressed in the form

$$M_w C_w \frac{dT_w}{dt} = C_i(T_i - T_w) + C_o(T_{amb} - T_w) + (\alpha RH) \qquad (3.4)$$

where $M_w C_w$ = effective thermal capacitance of the isothermal section

dT_w/dt = time rate of temperature change of the isothermal section

C_i = thermal conductance between the node of the isothermal section and the classroom interior

T_i = temperature of the interior

T_w = temperature of the isothermal section

C_o = thermal conductance between the node of the isothermal section and the exterior

T_{amb} = ambient temperature

(αRH) = heat gain due to incident solar radiation

The interior of the classroom is modeled as a single node. The effective thermal capacitance of the interior is the sum total of the thermal capacitances of the floor, interior walls, and the air in the building. The governing differential equation describing the energy balance of the interior is (4):

$$M_i C_i \frac{dT_i}{dt} = Q_{wn} + Q_{ww} + Q_{ws} + Q_{we} + Q_r + Q_f + Q_d + Q_{rad} + Q_{wd} + Q_i + Q_p + Q_e$$

$$+ Q_{cl} + Q_{aux} \qquad (3.5)$$

where $M_i C_i$ = effective thermal capacitance of the interior

dT_i/dt = time rate of change of temperature of the interior

All the "Q" terms represent heat gains and losses to the interior of the classroom due to:

1. Q_{wn}, Q_{ww}, Q_{ws}, Q_{we}, Q_r are heat transfers to the interior by conduction through the north, west, south, and east walls and the roof, respectively. In the general form, the rate of heat transfer is given by

$$Q_w = A_w C_i (T_w - T_i) \qquad (3.6)$$

where A_w = area of the wall

C_i = thermal conductance between the node of the wall and the interior

T_w = nodal temperature of the wall

T_i = nodal temperature of the interior

2. Q_f, Q_d are heat transfers to the interior by conduction through the floor and door and can be described by the rate equation 3.6. However, C_i has to be replaced by an overall thermal conductance for the partition, and T_w is assumed to be $25^{\circ}C$, the temperature in the next room.

3. Q_{rad} is heat gain due to radiation through the unshaded protion of the windows. The general form of the energy rate equation is

$$Q_{rad} = A_{wd} S c H R \tau_{wd} \qquad (3.7)$$

where A_{wd} = area of the window

Sc = shade factor, which represents the portion of the window that is exposed to direct sun light

HR = solar radiation on a titled surface

τ_{wd} = transmittance of the window glass

4. Q_{wd} is the rate of heat transfer due to conduction through all the windows and is given by

$$Q_{wd} = A_{twd} U_{wd} (T_{amb} - T_i) \qquad (3.8)$$

where A_{twd} = total window area

U_{wd} = overall conductance of the window glass

T_{amb} = ambient temperature

5. Q_i is the rate of heat gain due to infiltration of outside air. The rate is given by

$$Q_i = R_C V_R C_{air} (T_{amb} - T_i) \qquad (3.9)$$

where V_R = volume of the classroom interior

R_C = rate of air volume changes

C_{air} = capacitance of air, (density x specific heat)

6. Q_p, Q_e are respectively, heat gains due to people and lighting fittings. The instantaneous rate of heat gain from electric light fittings (3) is given by the equation:

$$Q_e = W \times UF \times AF \qquad (3.10)$$

where W = total rated light wattage of all fittings

UF = use factor, which depends upon the proportion of the total light wattage actually in use at time of load calculation (1 for commercial application)

AF = allowance factor, 1.2 for fluorescent fittings

The rate of heat gain from the occupants, Q_p, in the classroom is assumed to be 0.07 kW per person (3). This corresponds to a degree of activity where the person is seated with very light work.

7. Q_{cl} is the rate of heat transfer between the fan-coil unit and the interior air. Q_{cl} is determined by the fan-coil model.

8. Q_{aux} is the rate of heat transfer to the interior by auxiliary means.

The fan-coil unit provides a small degree of air conditioning. In order to analyze the dehumidification process occurring in the fan-coil unit, the moisture content of the air in the classroom is needed. The moisture content is described by the term, specific humidity S_i, which is defined as the mass of water per kg mass of air. A mass balance describing the variation of moisture content in the interior of the classroom with time is

$$M_A \frac{dS_i}{dt} = G_i + G_p + G_{cl} \qquad (3.11)$$

where M_A = mass of air in the classroom

dS_i/dt = time rate of change of the specific humidity of air in the classroom interior

G_i = rate of moisture gain due to infiltration

G_p = rate of moisture gain due to vaporization from occupants

= 0.0004 kg/s (3)

G_{cl} = rate of moisture removal by the fan-coil unit

The rate of moisture gain due to infiltration is given by

$$G_i = R_C V_R \rho (S_{amb} - S_i) \qquad (3.12)$$

where $R_C V_R$ = rate of infiltration of air

ρ = density of air

S_{amb} = specific humidity of ambient air

Fan-Coil Unit

The heat exchange between the air in the classroom interior and the solar system heat transfer medium, water, is accomplished by a 11.1 kW fan-coil unit. Specifications and performance data are presented in Appendix B.

Curve fitting of the performance data produced an unique relation for the coil heat transfer coefficient-area product, UA, as a function of a ratio of sensible to total heat transfer rate. The total heat transfer rate is the sum of sensible heat and latent heat. For heating operation the latent heat term can be omitted. The equation is in the form of

$$UA = 830.97 - 92.26\ R_Q + 178.98\ R_Q^2 \qquad (3.13)$$

where UA = heat transfer coefficient-area product, $W/^oC$

R_Q = ratio of sensible to total heat transfer rate

For heating operation, UA is 917.69 $W/^oC$. In addition, a relation for the change in specific humidity of air passing through the coil as a function of R_Q was also obtained.

$$\Delta S = + 0.0048179 - 0.0046635\ R_Q^{-1} \qquad (3.14)$$

In this equation, R_Q^{-1} must be greater than 1.03 because ΔS can never have a positive value, i.e., an increase in moisture content for air

passing through the coil.

The ratio of sensible to total heat removal or addition in the coil is given by the equation:

$$R_Q = \frac{-(\alpha + a\beta) + \sqrt{(\alpha + a\beta)^2 + 4b\beta\gamma}}{2b\beta} \qquad (3.15)$$

The variables α, β, γ, a and b are defined as follows:

$$a = -0.0048179$$

$$b = 0.0046635$$

$$\alpha = (1 + 1.86S_i)(T_{di} - T_{do})$$

$$\beta = 2500 + 1.86T_{do}$$

$$\gamma = 1.02(T_{di} - T_{do})$$

where

T_{di} = inlet air dry-bulb temperature

T_{do} = outlet air dry-bulb temperature

Derivation of equation 3.15 is presented in Appendix B.

The fan-coil unit is modeled as a counter-flow heat exchanger. The outlet temperatures of the two heat exchanging streams can be determined by the following equations (18):

For the hot stream,

$$T_{ho} = T_{hi} - (T_{hi} - T_{ci})\frac{E_c}{E_h}(1 - f) \qquad (3.16)$$

For the cold stream,

$$T_{co} = T_{hi} - (T_{hi} - T_{ci})\, f \qquad (3.17)$$

and f is given by the expression

$$f = \frac{1 - \frac{E_h}{E_c}}{1 - \frac{E_h}{E_c} \exp\left[- UA(1 - E_h/E_c)/E_h \right]} \qquad (3.18)$$

where

T_{ho} = outlet temperature of the hot stream

T_{hi} = inlet temperature of the hot stream

T_{co} = outlet temperature of the cold stream

T_{ci} = inlet temperature of the cold stream

E_h = water equivalent of the hot stream, (mass flow rate x specific heat)

E_c = water equivalent of the cold stream

UA = = heat transfer coefficient-area product

For cooling operation, the process for calculating the heat exchange rate is a repetitive one, since UA is related to R_Q which is a function of the outlet air temperature. To begin the calculation, an UA is assumed so that an outlet air temperature can be determined from equation 3.16. Having the outlet air temperature permits the calculation of R_Q and subsequently, the UA product. If the difference between the calculated UA product and the assumed value is within a desired tolerance, the process is stopped and the UA product is determined; otherwise, the process is repeated with the newly calculated UA product.

For heating operation, the process for calculating the heat exchange rate is straightforward. No repeated calculation is required because the UA product is set at one value.

Thermal Storage Tanks

The mathematical model for each thermal storage tank, hot and chilled water, is a non-stratified, single node model, i.e., the water in each tank is at one uniform temperature. In a real system, stratification may occur and would improve the performance of the solar system due to lower collector inlet fluid temperatures. Therefore, a non-stratified storage system is a conservative representation of the actual system.

The equation describing the energy balance on the water in each storage tank accounts for the net energy gain or reduction from the inlet and outlet flows, and energy loss to the surroundings. The governing differential equation is

$$M_s C_p \frac{dT_s}{dt} = W_s C_p (T_{in} - T_s) + Q_\ell \qquad (3.19)$$

where

$M_s C_p$ = thermal capacitance of the water in the storage tank

dT_s/dt = time rate of change of storage water temperature

W_s = mass flow rate of water to or from the storage tank

C_p = specific heat of water

T_{in} = inlet water temperature to the storage tank

T_s = temperature of water in the storage tank

Q_ℓ = thermal loss from the storage tank to surroundings

Thermal loss from the storage tank to the surroundings is given by

$$Q_\ell = U_\ell A_s (T_s - T_{amb}) \qquad (3.20)$$

where U_ℓ = overall heat transfer coefficient between the storage tank and outside air

A_s = surface area of the storage tank

T_{amb} = ambient air temperature

Absorption Chiller

The chiller is a lithium bromide absorption unit. It uses directly the energy collected by the collector array or energy stored in the hot storage tank to generate chilled water. Performance data for this unit is presented in Appendix C.

The chiller is modeled as a "black box". From the performance data given, curve fitting provided a relation for the delivered capacity as a function of entering hot water temperature at an inlet condensing water temperature of 29.4°C.

$$Cap = -10.7922282 + 0.2138654\ T - 0.0009239\ T^2 \quad (3.21)$$

where Cap = delivered chilled water capacity expressed as a fraction of the design delivered capacity

T = temperature of entering hot water, °C

An empirical relation for the chiller's coefficient of performance, ratio of delivered capacity to input energy, as a function of entering hot water temperature was also obtained.

$$Cop = -14.7688242 + 0.3500924T - 0.0019752T^2 \quad (3.22)$$

where the entering hot water temperature is again expressed in °C.

CHAPTER IV

SOLAR RADIATION AND WEATHER DATA

Hourly solar radiation and weather data are essential to the computer simulations of transient solar systems. When hourly solar radiation data are not available, a method for predicting them must be provided. Since the incident solar radiation strikes surfaces of interest, most of which are non-horizontal, a method for converting the radiation data on a horizontal surface to those on a tilted surface must also be considered.

For the present study the 1964 solar radiation and weather data were used. Hourly relative humidity, air d-b temperature, and wind speed were obtained from the U. S. Weather Bureau Local Climatological Data for Atlanta. Hourly insolation values on a horizontal surface are available at Georgia Tech and were computed from the 1964 Weather Service Cloud Cover Data for Atlanta.

Solar Radiation

Solar radiation on a flat-plate collector consists of two components: beam and diffuse. The estimation of the quantity of each component is required for the computation of the actual rate of incident solar radiation on the collector.

Estimation of Hourly Diffuse Radiation

A simple method for estimating the hourly diffuse radiation on a horizontal surface from the daily total radiation has been developed by

Liu and Jordan (15). This method consists of two steps: first, daily diffuse radiation is estimated from the daily total; second, hourly diffuse is estimated from the calculated daily diffuse.

The relation between daily diffuse radiation and daily total radiation is shown in Figure 6 as an unique function of a cloudiness index, i.e., a ratio of daily total radiation to daily extraterrestrial radiation. Curve fitting of this relation resulted in an equation of the form

$$K_D = 0.9963736 + 0.0972454K_T - 3.7281838K_T^2 + 2.8696926K_T^3 \tag{4.1}$$

and K_D and K_T are defined as follows:

$$K_D = \frac{H_{DD}}{H_{DT}}$$

$$K_T = \frac{H_{DT}}{H_{DE}}$$

where H_{DD} = daily diffuse radiation on a horizontal surface

H_{DT} = daily total radiation on a horizontal surface

H_{DE} = daily extraterrestrial insolation on a horizontal surface

The hourly diffuse radiation is related to the daily diffuse by the equation:

$$r_d = \frac{\pi}{24} \frac{\cos \omega - \cos \omega_s}{\sin \omega_s - \omega_s \cos \omega_s} \tag{4.2}$$

where r_d = ratio of hourly diffuse to daily diffuse radiation

ω = hour angle, degrees (solar noon being zero and

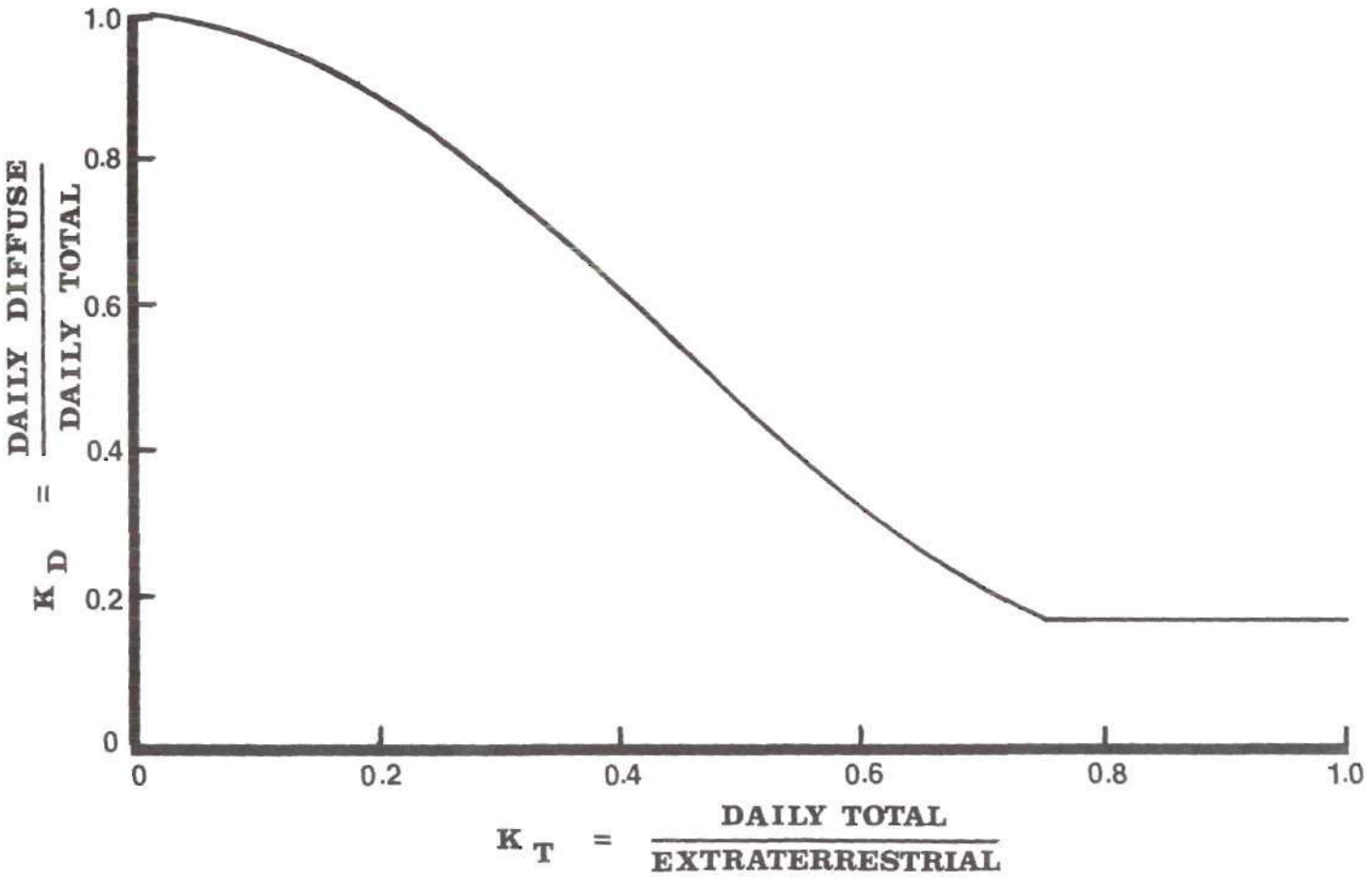

Figure 6. Ratio of Daily Diffuse Radiation to Daily Total Radiation

each hour equaling 15^{o} of longitude with morning positive and afternoon negative, e.g., $\omega = +15$ for 11:00, and $\omega = -37.5$ for 14:30)

ω_s = sunset hour angle, radians

The sunset hour angle, ω_s, is given by (6):

$$\omega_s = \frac{\pi}{180} \cos^{-1}\left\{- \tan\phi \tan\left[23.4 \sin\left(\frac{360(284 + n)}{365}\right)\right]\right\} \quad (4.3)$$

where ϕ = latitude (north positive)

n = the day of the year

Estimation of Hourly Total Radiation

If only the total daily radiation on a horizontal surface is available, hourly total radiation may be estimated from the experimental ratio of hourly total radiation to daily total radiation plotted in Figure 7 (15). In addition, equations for these relations derived from curve fitting are also given in Table 1.

Ratio of Total Radiation on a Tilted Surface to That on a Horizontal Surface

The total radiation on a tilted surface consists of three components: beam, diffuse, and reflected solar radiation from the ground which the tilted surface "sees". The hourly ratio of total radiation on a tilted surface to that on a horizontal surface is given by (6):

$$R = \frac{H_b}{H_T} R_b + \frac{H_d}{H_T} \frac{(1 + \cos s)}{2} + \frac{(1 - \cos s)\rho}{2} \quad (4.4)$$

where H_b = hourly beam radiation on a horizontal surface

H_T = hourly total radiation on a horizontal surface

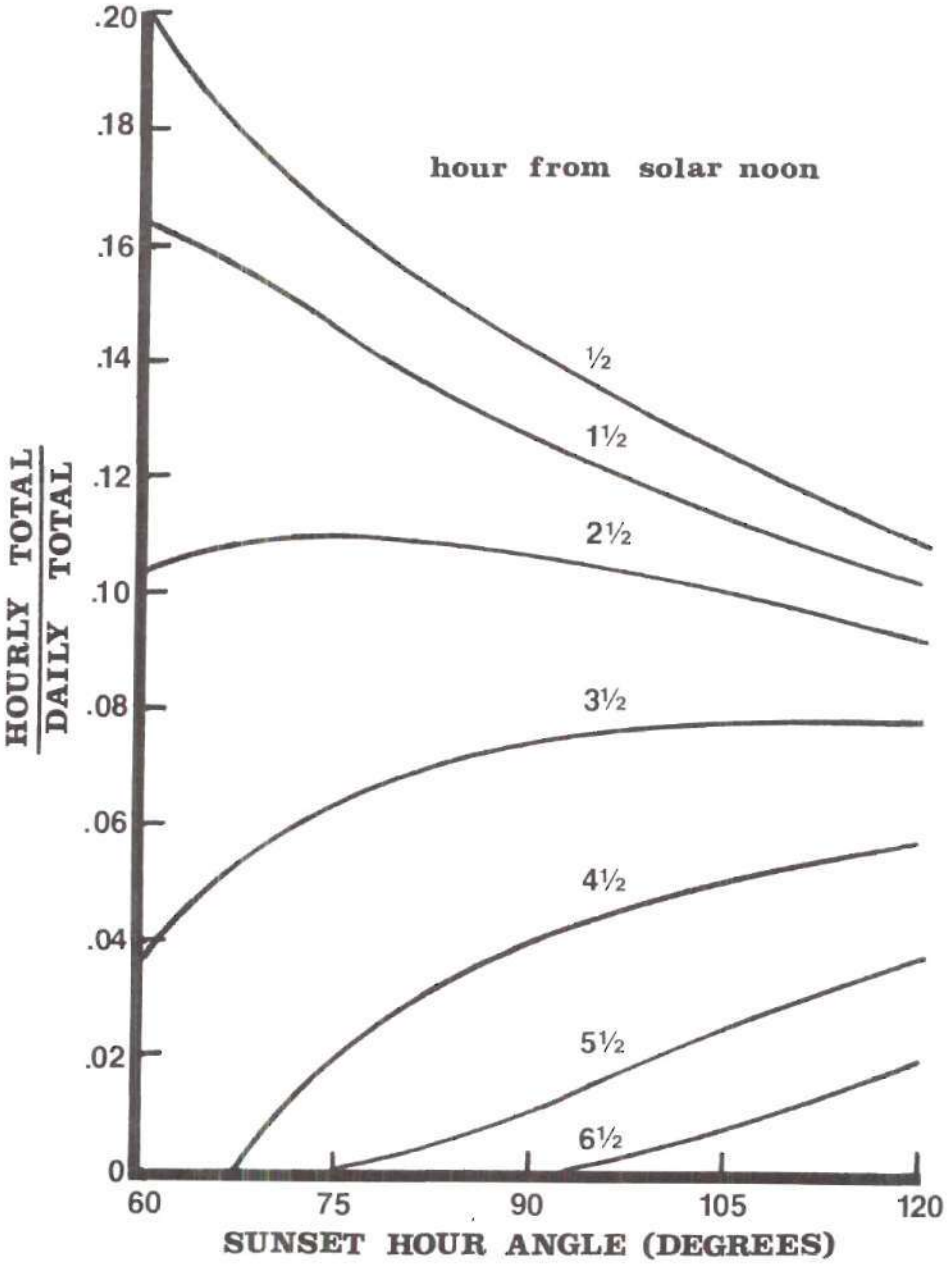

Figure 7. Experimental Ratio of Hourly Total Radiation to Daily Total Radiation

Table 1. Experimental Ratio of Hourly Total Radiation to Daily Total Radiation

General form of the equation:

$$r_T = A + B\omega_S^2 + C\omega_S^2$$

Hour From Noon	A	B	C
½	0.4066000	- 0.0045467	0.0000178
1½	0.2717000	- 0.0021933	0.0000067
2½	0.0193500	0.0022700	- 0.0000144
3½	- 0.2198000	0.0061067	- 0.0000311
4½	- 0.1190554	0.0022826	- 0.0000061
5½	0.0374600	- 0.0012747	0.0000107
6½	0.0409500	- 0.0011433	0.0000078

H_d = hourly diffuse radiation on a horizontal surface

R_b = ratio of beam radiation on a tilted surface to that on a horizontal surface

s = slope of the surface from the horizontal

η = ground reflectance (suggested values of 0.2 when there is no snow and 0.7 when there is snow)

The ratio of beam radiation on a tilted surface to that on a horizontal surface, R_b, is defined by

$$R_b = \frac{\cos(\theta_T)}{\cos(\theta_z)} \tag{4.5}$$

where θ_T = the angle between incident beam radiation and normal to the surface

θ_z = the angle between incident beam radiation and vertical

These angles are defined by

$$\cos(\theta_z) = \sin(\delta)\sin(\phi) + \cos(\delta)\cos(\phi)\cos(\omega) \tag{4.6}$$

and

$$\begin{aligned}\cos(\theta_T) = {} & \sin(\delta)\sin(\phi)\cos(s) \\ & - \sin(\delta)\cos(\phi)\sin(s)\cos(\gamma) \\ & + \cos(\delta)\cos(\phi)\cos(s)\cos(\omega) \\ & + \cos(\delta)\sin(\phi)\sin(s)\cos(\gamma)\cos(\omega) \\ & + \cos(\delta)\sin(s)\sin(\gamma)\sin(\omega)\end{aligned} \tag{4.7}$$

where δ = declination

γ = surface azimuth angle, zero being due south, east positive, and west negative

The declination, δ, can be found from the approximate equation of Cooper (5):

$$\delta = 23.45 \sin\left[360 \frac{(284 + n)}{365}\right] \tag{4.8}$$

where n is the day of the year.

Specific Humidity of Air

Atmospheric moisture content is usually expressed as relative humidity. Formulation of equations to convert relative humidity to specific humidity is necessary for the computation in the computer program. Specific humidity is defined as the mass of water per kg mass of air. Relative humidity, RH, is defined as

$$RH = \left(\frac{P_s}{P_d}\right)_{T_d} \tag{4.9}$$

where P_s = partial pressure of the water vapour in the air

P_d = pressure of saturated steam at the air temperature (dry-bulb temperature, T_d)

The pressure of the saturated steam at the air dry-bulb temperature is given by the equation (23):

$$P_d = \exp\left\{\frac{-G \sqrt{G^2 - 4FH}}{2F}\right\} \tag{4.10}$$

where P_d = saturated steam pressure at the air dry-bulb temperature, in (H_g)

$F = -0.07086745$

$G = 0.001626943T_d - 1.0$

$H = -0.00004286517T_d^2 + 0.03533457T_d - 2.519124$

T_d is in ^oF. Knowing P_d and RH, the partial pressure of water vapour in the air can be calculated from equation 4.9. The specific humidity of

air is related to the partial pressure of water vapour, P_s, by the equation:

$$S = 0.622 \frac{P_s}{(B_a - P_s)} \qquad (4.11)$$

where S = specific humidity, kg of water vapour per kg of air

B_a = barometric pressure

All pressure terms must be expressed in the same unit.

CHAPTER V

COMPUTER SIMULATION

Program Description

The computer program developed for the simulation of the multi-mode solar heating and cooling system is based on a modular approach, i.e., each system component can be mathematically described without regard to the other components. The program is composed of an "executive" program and seven subroutines, each models the function of a particular solar energy system component. In addition, two non-hardware modeling subroutines are used to provide hourly and instantaneous solar radiation and weather data.

A brief description of each program with corresponding flow chart is presented alphabetically in this chapter.

Atm

Atm is responsible for supplying to the rest of the program instantaneous solar radiation and weather data, and ratios of total radiation on a tilted surface to that on a horizontal surface for the south and west walls, roof, and the collector array.

Chill

Chill is a "black box" model of the absorption chiller. The component model is empirically defined by transfer functions obtained from curve fitting of performance data.

Coil

Coil is a modeling subroutine of the fan-coil unit. The program is divided into two subprograms: one for heating operation and the other for cooling. In the cooling operation, a repetitive process is used to calculate the heat transfer coefficient-area product, UA. For the heating operation UA is given.

Col

Col is a modeling subroutine of solar flat-plate collectors.

Contr

The primary task of the subroutine, Contr, is to facilitate the interconnection of system components in a fashion dictated by the selected mode of operation. It defines exactly how all component inputs and outputs are to be interconnected and transfers this information to the subroutines.

Load

Load is a modeling subroutine for the calculation of heating or cooling load of the classroom.

Main

Main is the "executive and the heart" of the computer program which controls the operation of the system by calling each subroutine at the appropriate time, and transfers information between the subroutines.

Main also serves as an integrator for the set of differential equations developed in Chapter III for the solar system components.

In addition, Main also selects the mode of operation, calculates component net heat transfer rates, and prints out the results. Figures 9 and 10 show the methods of mode selection.

Moist

Moist is a subroutine for determining the moisture content of air in the interior of the classroom.

Stor

Stor is a modeling subroutine of the hot and chilled water storages.

Wethr

One of the functions of Wethr is to convert input data to metric units: knots to m/s, ^{o}F to ^{o}C, and Btu/hft^2 to W/m^2. Also, relative humidity is converted to specific humidity. The primary function of Wethr is to determine the hourly diffuse solar radiation, the hourly total radiation, if required, and constants for interpolating intermediate values of the diffuse radiation, total radiation, wind speed, ambient air temperature, and specific humidity of air.

Method of Integration

The computer program uses a fourth order Runge-Kutta method for solving the system of first order ordinary differential equations. The process employs a constant step size of one minute interval for the independent variable, time. One minute step size was found to be sufficient to keep the truncation error at a value less than one hundredth of a percent.

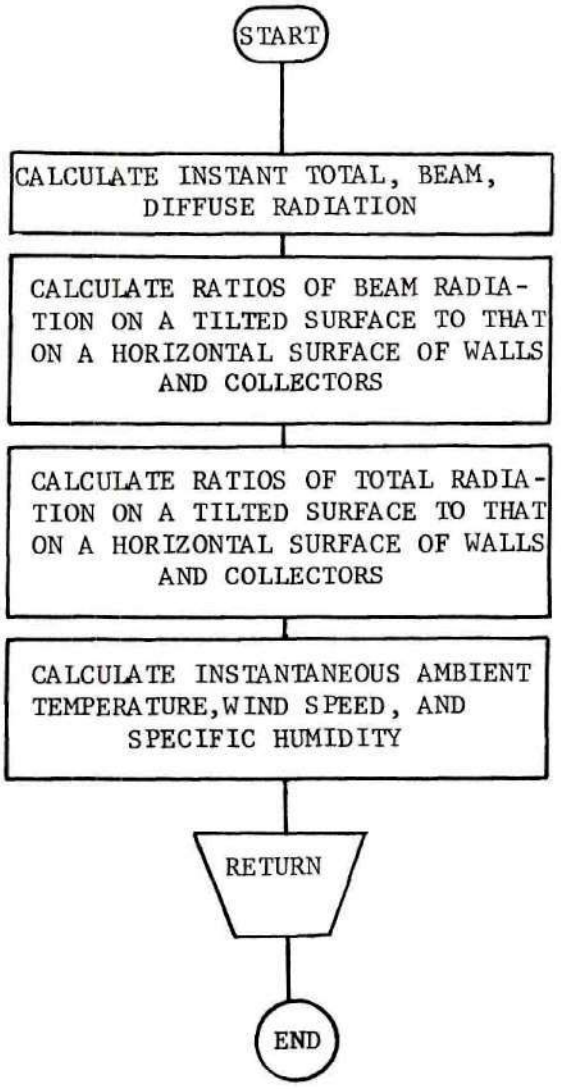

Figure 8a. Flow Chart of Atm

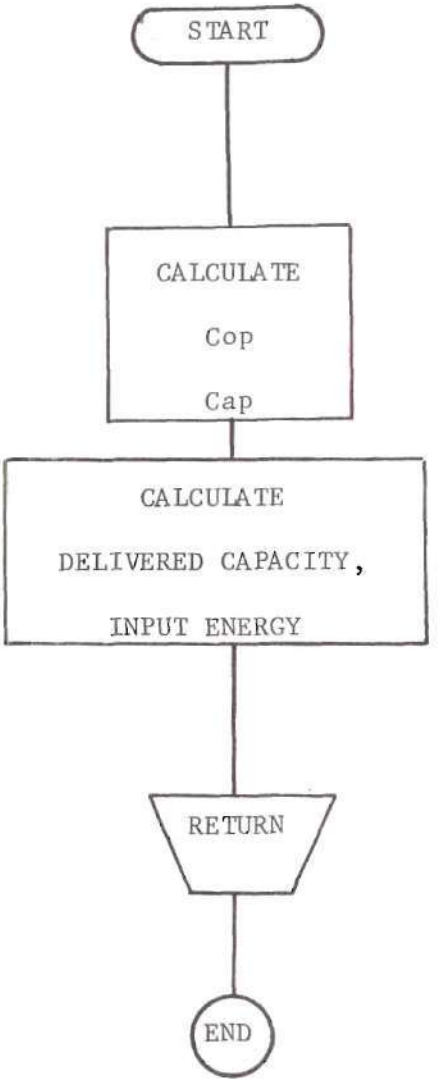

Figure 8b. Flow Chart of Chill

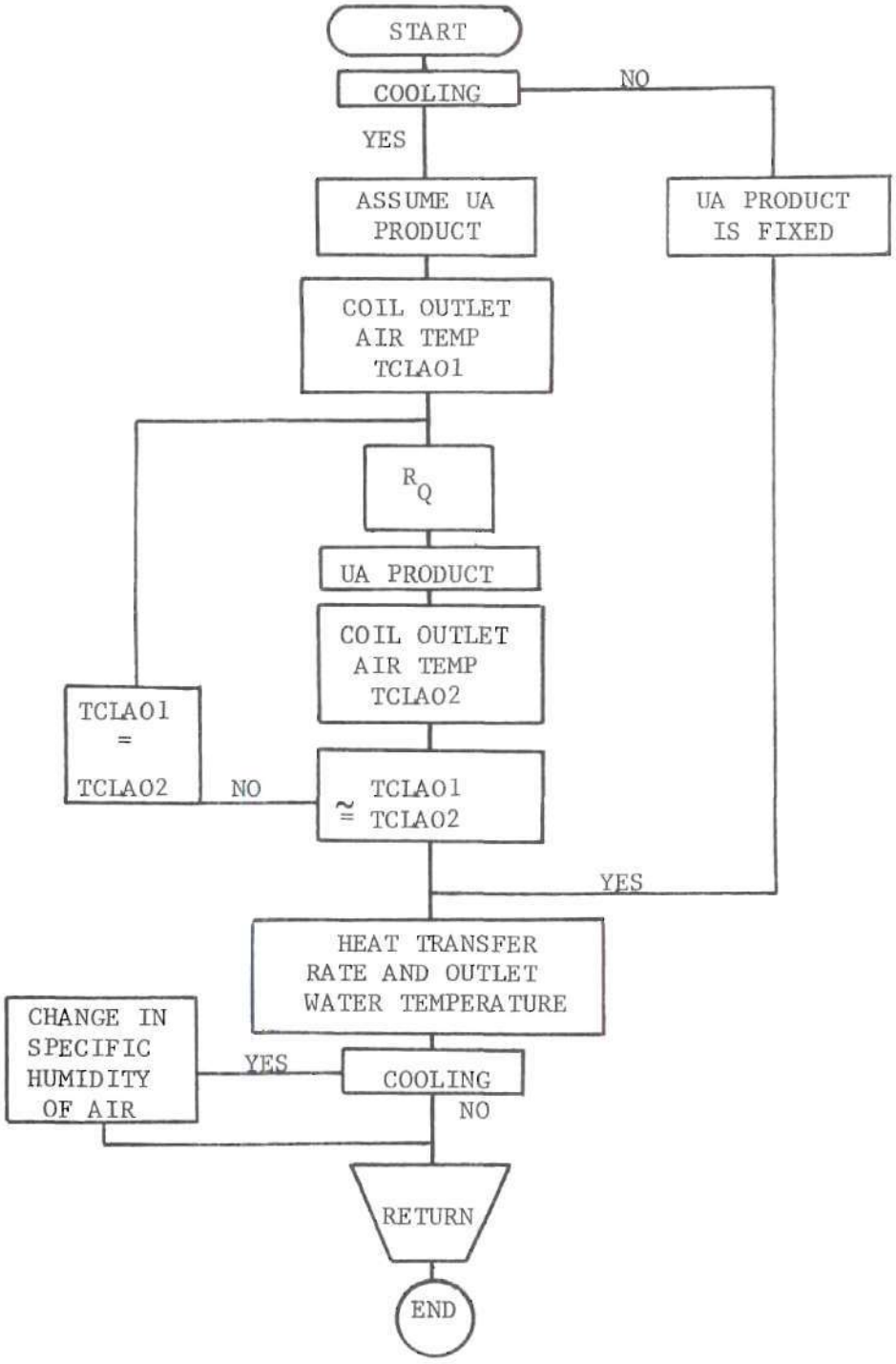

Figure 8c. Flow Chart of Coil

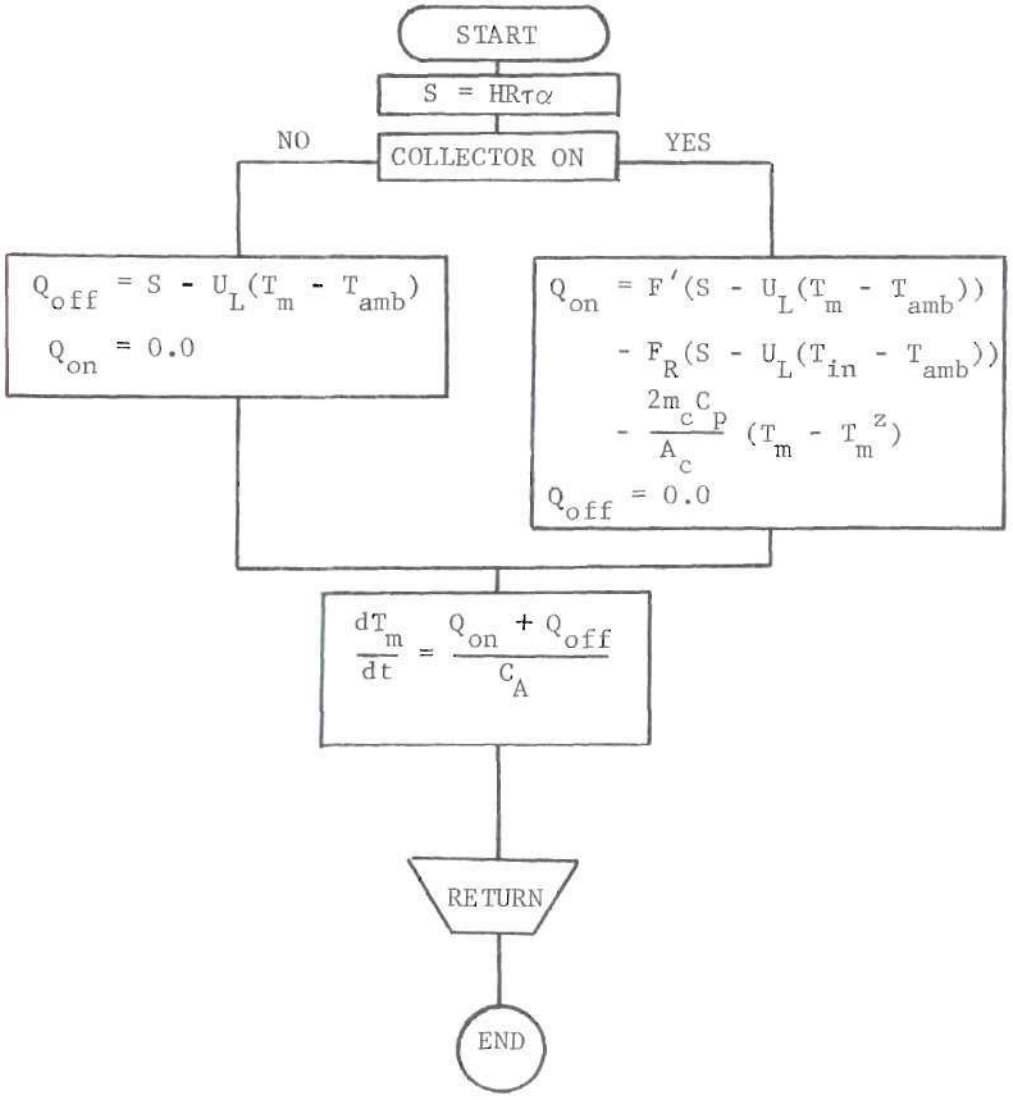

Figure 8d. Flow Chart of Col

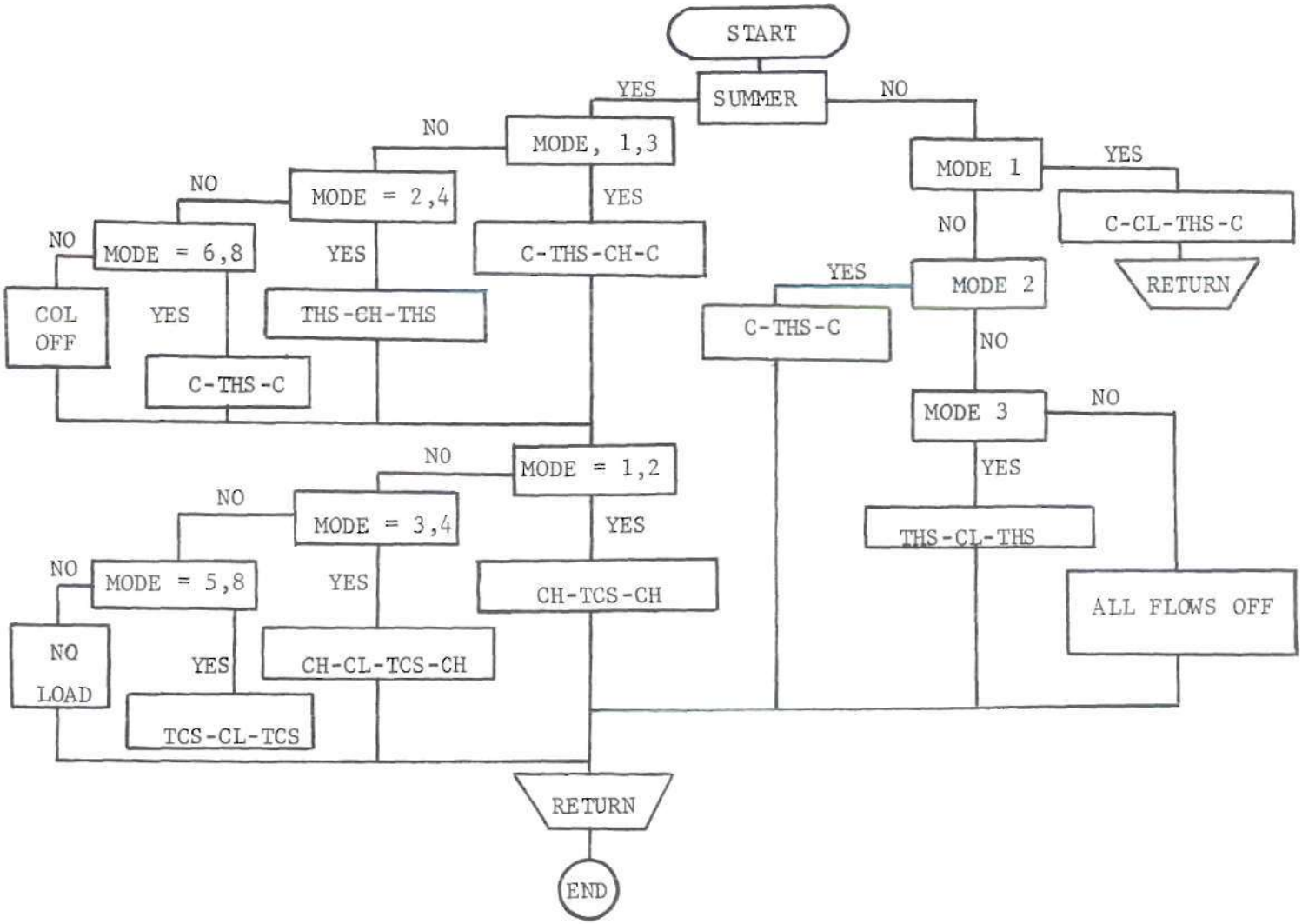

Figure 8e. Flow Chart of Contr

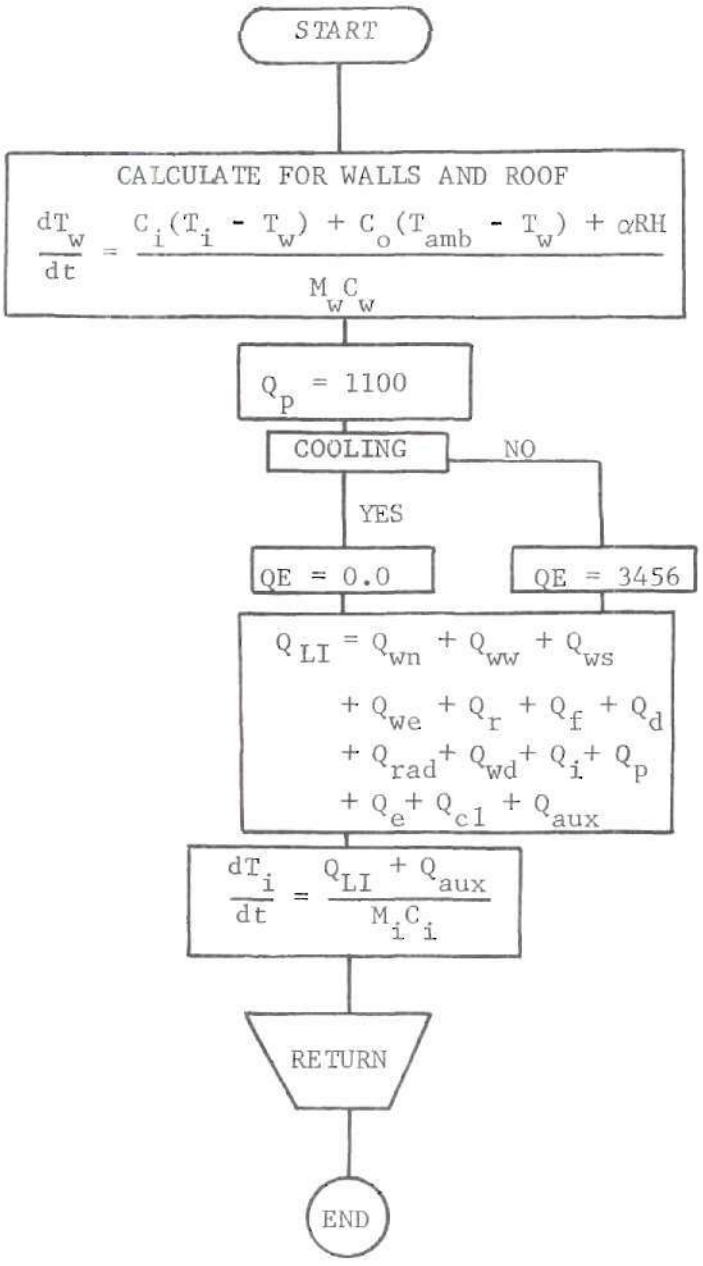

Figure 8f. Flow Chart of Load

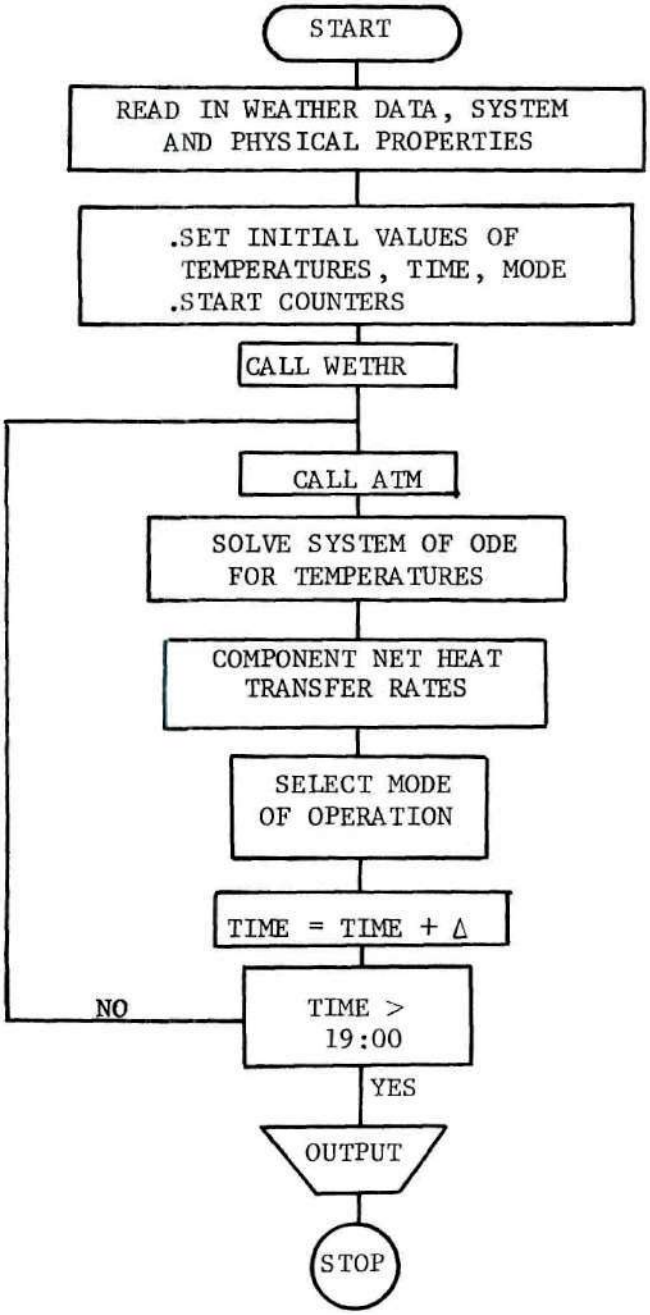

Figure 8g. Flow Chart of Main

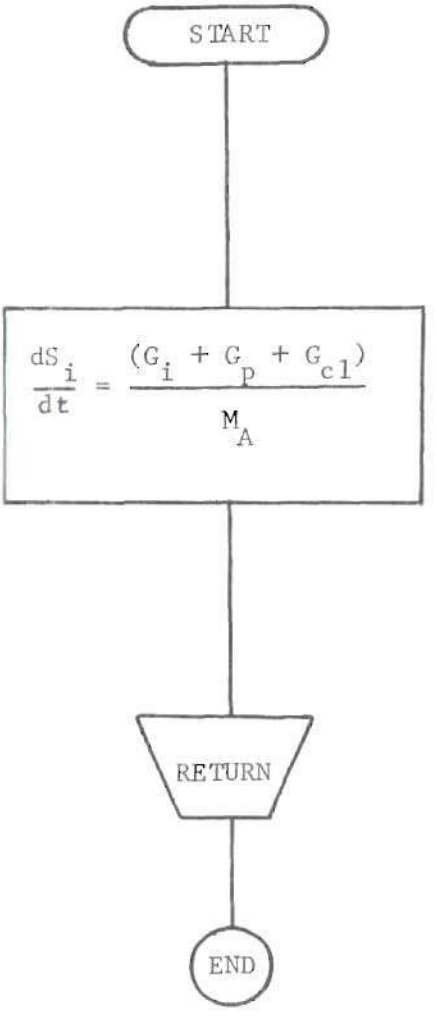

Figure 8h. Flow Chart of Moist

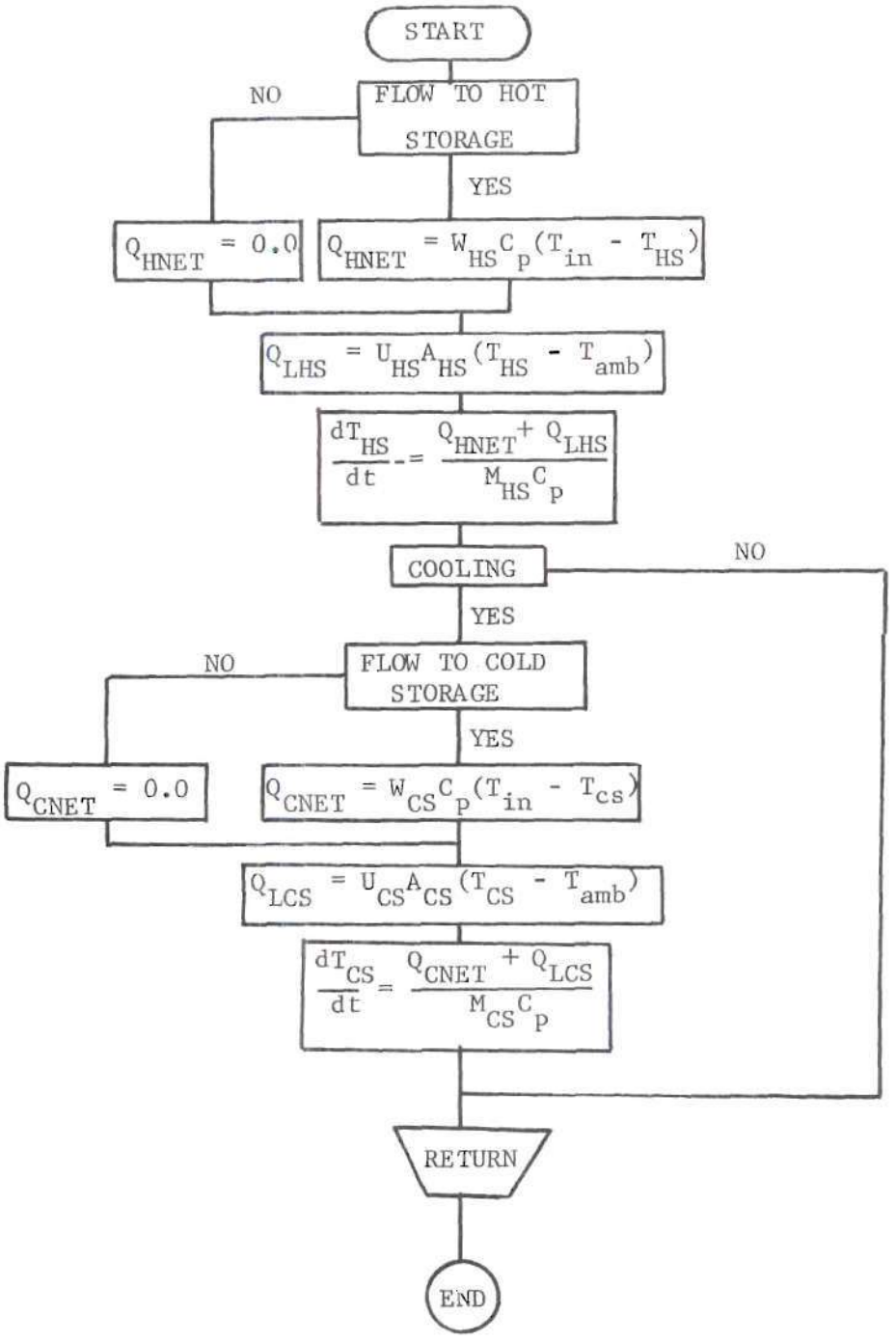

Figure 8i. Flow Chart of Stor

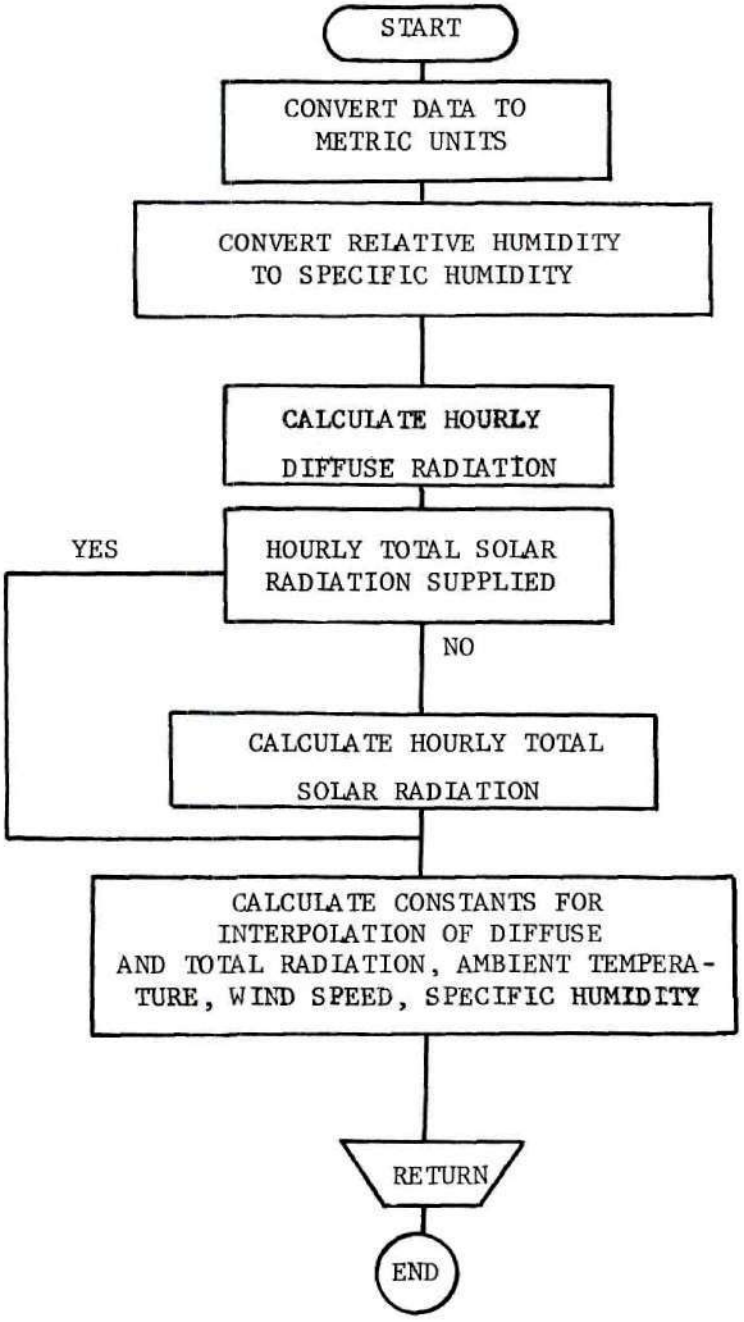

Figure 8j. Flow Chart of Wethr

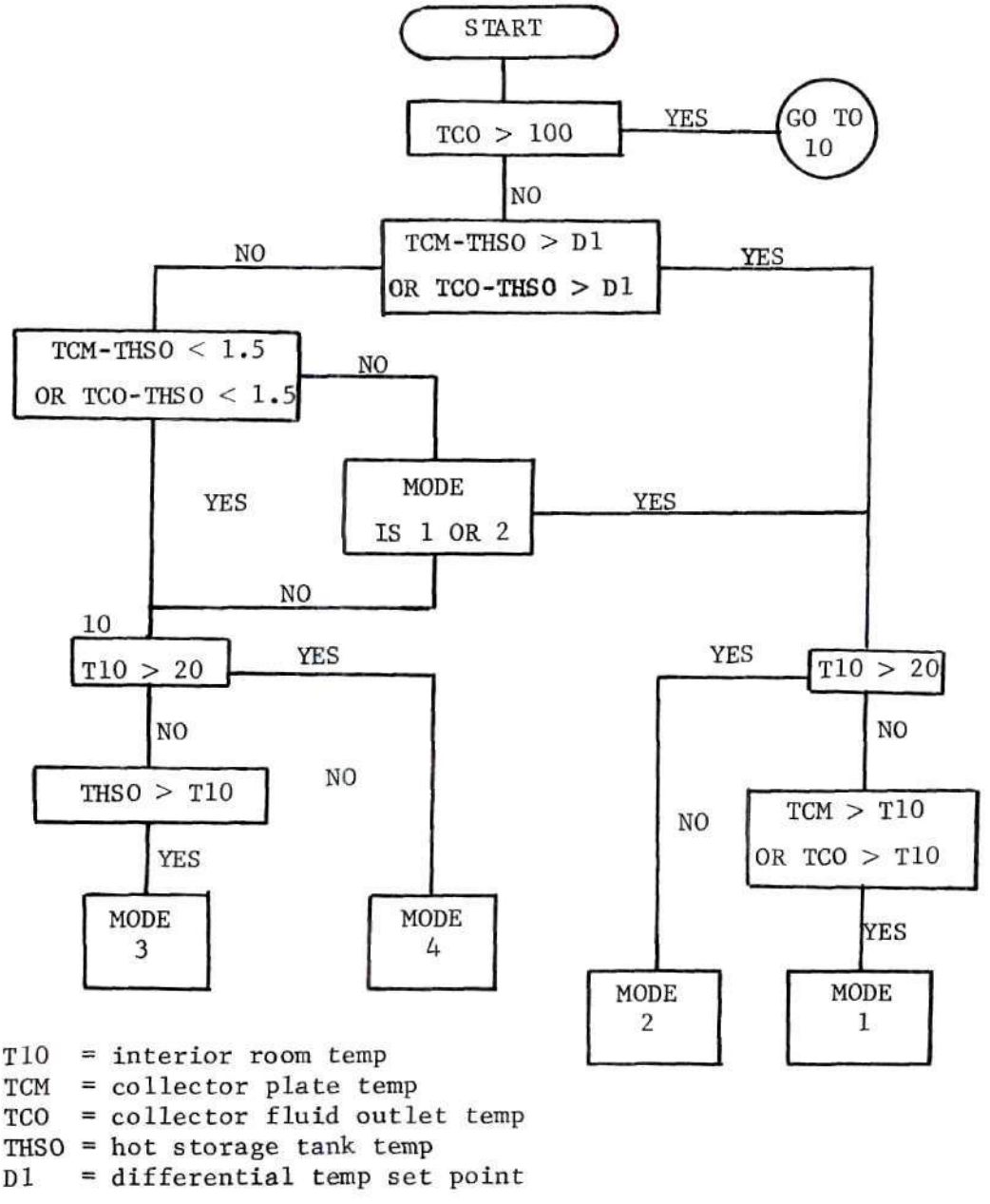

Figure 9. Mode Selection: Heating

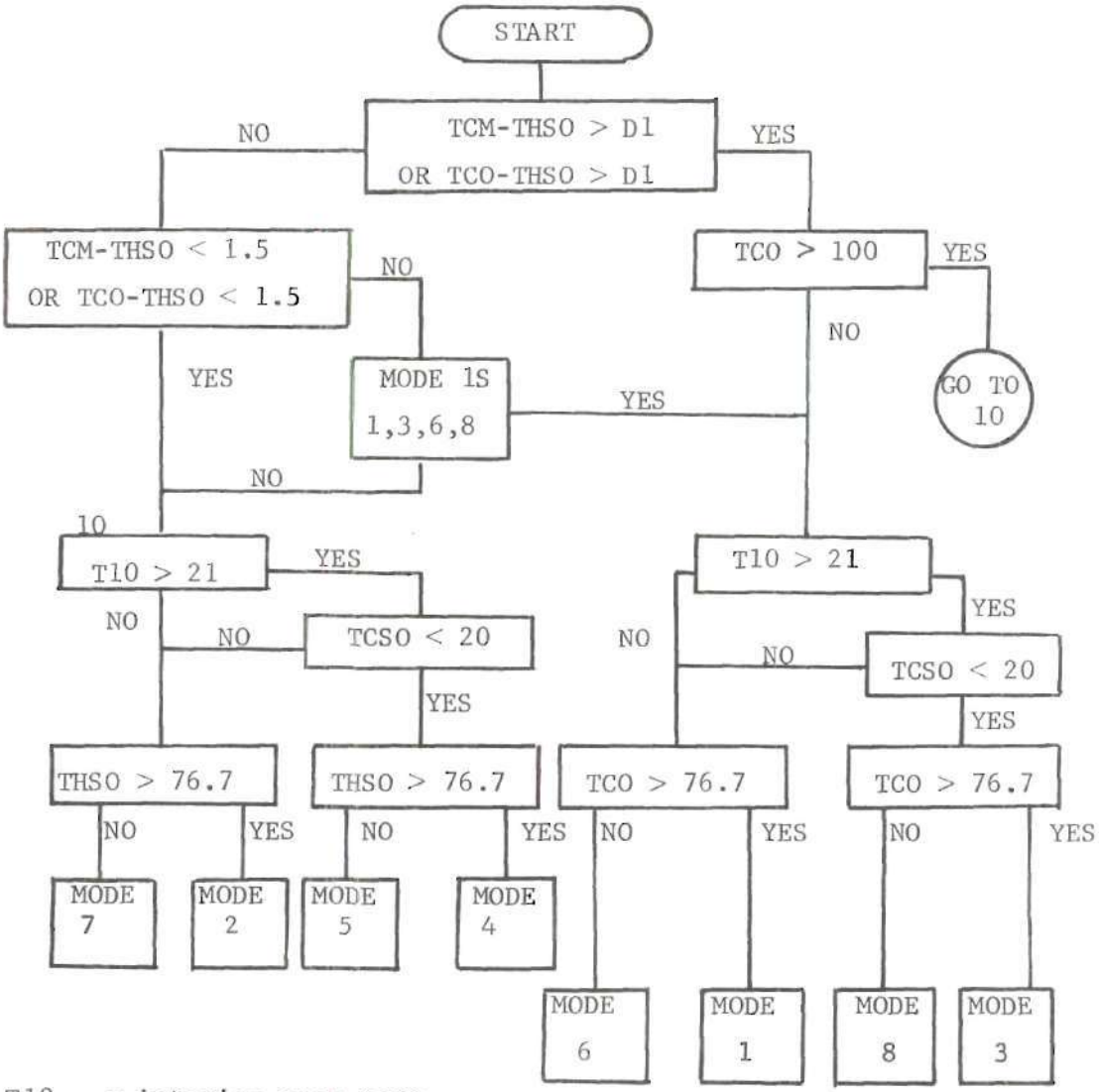

T10 = interior room temp
TCM = collector plate temp
TCO = collector fluid outlet temp
THSO = hot storage tank temp
D1 = differential temp set point

Figure 10. Mode Selection: Cooling

The error estimates were obtained by solving the system at two different step lengths (16): one at one minute interval, the other at half minute interval. The true value of each solution is given by

$$Y = y^{(h)} + E_T \tag{5.1}$$

where Y = true value

$y^{(h)}$ = value calculated with a step size h

E_T = truncation error.

The truncation error is given by

$$E_T = \frac{32}{31}\left[y^{(h/2)} - y^{(h)}\right] \tag{5.2}$$

where $y^{(h/2)}$ = value calculated with a step size of h/2

System Parameters

Values for the main parameters used in this study are given in Table 2. Some of these parametric values were fixed by the physical nature of the experimental system. The others were obtained from calculations and/or published literatures.

Table 2. System Parameters

Geographical Data		
Latitude	ϕ	$= 33.5^{o}$
Flow Rates and Properties		
Specific heat of water	Cp_w	$= 4.19 \times 10^3$ J/kg ^{o}C
Specific heat of air	Cp_a	$= 1.01 \times 10^3$ J/kg ^{o}C
Density of Air	ρ	$= 1.204$ kg/m^3
Hot water flow rate	m_{hot}	$= 0.694$ kg/s max.
Chilled water flow rate	m_{cold}	$= 0.454$ kg/s design
Air volume thru fan-coil	m_{air}	$= 0.680$ kg/s design
Building		
Effective thermal capacitance of walls	$M_w C_w$	$= 5.31 \times 10^5$ J/m^2 ^{o}C
Effective thermal capacitance of roof	$M_R C_R$	$= 1.56 \times 10^5$ J/m^2 ^{o}C
Effective thermal capacitance of the interior	$M_i C_i$	$= 3.67 \times 10^6$ J/^{o}C
Thermal conductance between wall node and interior	$(C_i)_w$	$= 4.1$ W/m^2 ^{o}C
Thermal conductance between wall node and ext. excluding ext. surface conductance	$(C_o)_w$	$= 4.5$ W/m^2 ^{o}C
Thermal conductance between roof node and interior	$(C_i)_r$	$= 0.97$ W/m^2 ^{o}C
Thermal conductance between roof node and ext. excluding ext. surface conductance	$(C_o)_r$	$= 1.27$ W/m^2 ^{o}C

Table 2. (Continued)

Overall conductance of east wall	U_{we}	= 1.76 $W/m^2\ ^oC$
Overall heat transfer coefficient of floor	U_f	= 1.31 $W/m^2\ ^oC$
Overall heat transfer coefficient of door	U_d	= 1.79 $W/m^2\ ^oC$
Overall conductance of window glass	U_w	= 6.25 $W/m^2\ ^oC$
Area of roof	A_r	= $122m^2$
Area of floor	A_f	= $122m^2$
Area of door	A_d	= $3.3m^2$
Area of north wall	A_{wn}	= $34.2m^2$
Area of west wall	A_{ww}	= $29.5m^2$
Area of south wall	A_{ws}	= $22.2m^2$
Area of east wall	A_{we}	= $49.1m^2$
Area of south wall windows	$(A_{wd})_s$	= $12m^2$
Area of west wall windows	$(A_{wd})_w$	= $19.6m^2$
Mass of air in the interior	M_A	= 545 kg
Volume of the interior of classroom	V_R	= $453m^3$
Rate of heat transfer by auxiliary cooler	Q_{aux}	= 10.5 kW max. assumed
Shade factor of windows	Sc	= 1.0
Transmittance of window glass	τ_{wd}	= 0.86
*Rate of air volume changes (3)	R_c	= $4.2 \times 10^{-4}\ s^{-1}$
Heat gain due to lighting fittings	Q_e	= 3.5 kW for heating, 0kW for cooling
Heat gain due to people	Q_p	= 1.1 kW
Room temperature setting	$(T_i)_{set}$	= 21^oC

Table 2. (Continued)

Storage Tanks		
Mass of hot storage water	$(M_S)_{hot}$	= 7277 kg max.
Mass of chilled storage water	$(M_S)_{cold}$	= 7277 kg max.
Overall heat transfer coefficient area-product between tank (hot or cold) and outside air	$U_\ell A_S$	= 4.32 W/^{o}C
Chiller		
Rated delivered capacity of chiller	Rate	= 10.5 kW
*Absorptivity of roof and walls for solar radiation (20)	α	= 0.7
Collectors		
*Lumped value of collector capacitance (7)	C_A	= 9.2 x 10^3 J/m^2 ^{o}C
Product of cover transmittance and plate absorptance	$\tau\alpha$	= 0.80
Collector overall loss coefficient	U_L	= 7.6 W/m^2 ^{o}C assumed
*Collector efficiency factor (7)	F'	= 0.97
*Collector heat removal factor (7)	F_R	= 0.95
Area of collector array	A_c	= 74.3m^2
Slope of collector array	s	= 45^{o}
Temperature difference between collector outlet fluid and hot storage tank required to initiate flow	$(\Delta T_C)_{upper}$	= varied for optimization study
Temperature difference between collector outlet fluid and hot storage tank required to turn off flow	$(\Delta T_c)_{lower}$	= 1.5 ^{o}C

*Values obtained from published literatures.

CHAPTER VI

DISCUSSION OF RESULTS

Program Evaluation

Several assumptions were made in the computer simulation of the multi-mode solar heating and cooling system. The main assumptions are as follows:

1. Constant physical properties of specific heat, density, and heat transfer coefficient,

2. assumed structures for the walls, roof, and the interior of the classroom,

3. assumed values for shade factor of windows, rate of air volume changes, and heat gains from people and lighting fittings,

4. assumed auxiliary cooling, and

5. assumed constant collector overall loss coefficient.

In the temperature range that the solar system operates, the assumption of constant physical properties is a good approximation.

However, the assumptions of classroom structural characteristics and values affecting the thermal behavior of the classroom provide only a conservative representation of the actual system. For example, the interior classroom temperature toward the end of the day as shown in Figure 11a is much higher than anticipated for heating operation.

The assumption of auxiliary cooling is necessary for cooling operation to maintain the interior classroom temperature within a reason-

able range, since the solar system can not meet 100% of the cooling load demand.

In a real system, the collector overall loss coefficient is a function of wind speed, plate absorptance and temperature, and the number of cover plates. For the majority of the collectors in the array, the assumed value for the collector overall loss coefficient is adequate for predicting the collector performance. For collector with selective coatings, the prediction would be a conservative one.

Examples of the computer results are plotted in Figures 11a,b,c and 12a,b, and c. The computer program prints out all pertinent temperature profiles and component net heat transfer rates.

The effect of thermal lag of solar radiation absorbed by the exterior walls on the interior temperature is clearly illustrated in Figure 12a. The solar radiation absorbed by the walls in the form of heat during the day is released in the evening and causes the interior classroom temperature to rise above the ambient air temperature.

Parametric Studies

Parametric studies of component and control parameters were carried out to determine their effects on system performance. Parametric values which prove to be most effective in increasing system performance could then be incorporated into control strategies: strategies that would operate the solar system in an optimized manner.

Solar insolation and weather data for eight selected days in 1964 for Atlanta were used in these studies: January 13 and 14, March 9, April 15, June 22 and 25, September 14, and October 1. Weather conditions

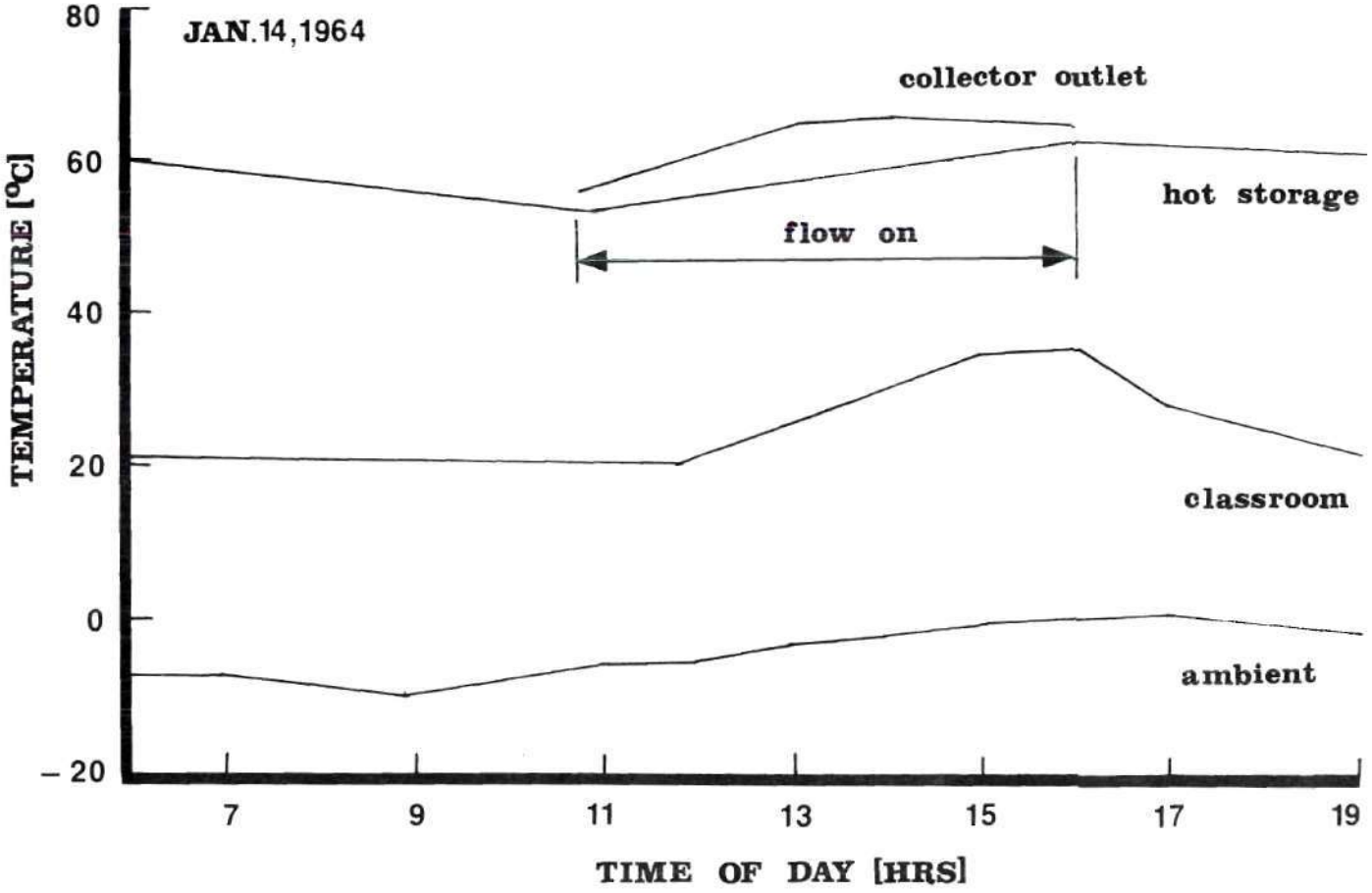

Figure 11a. Temperature Profiles: Heating

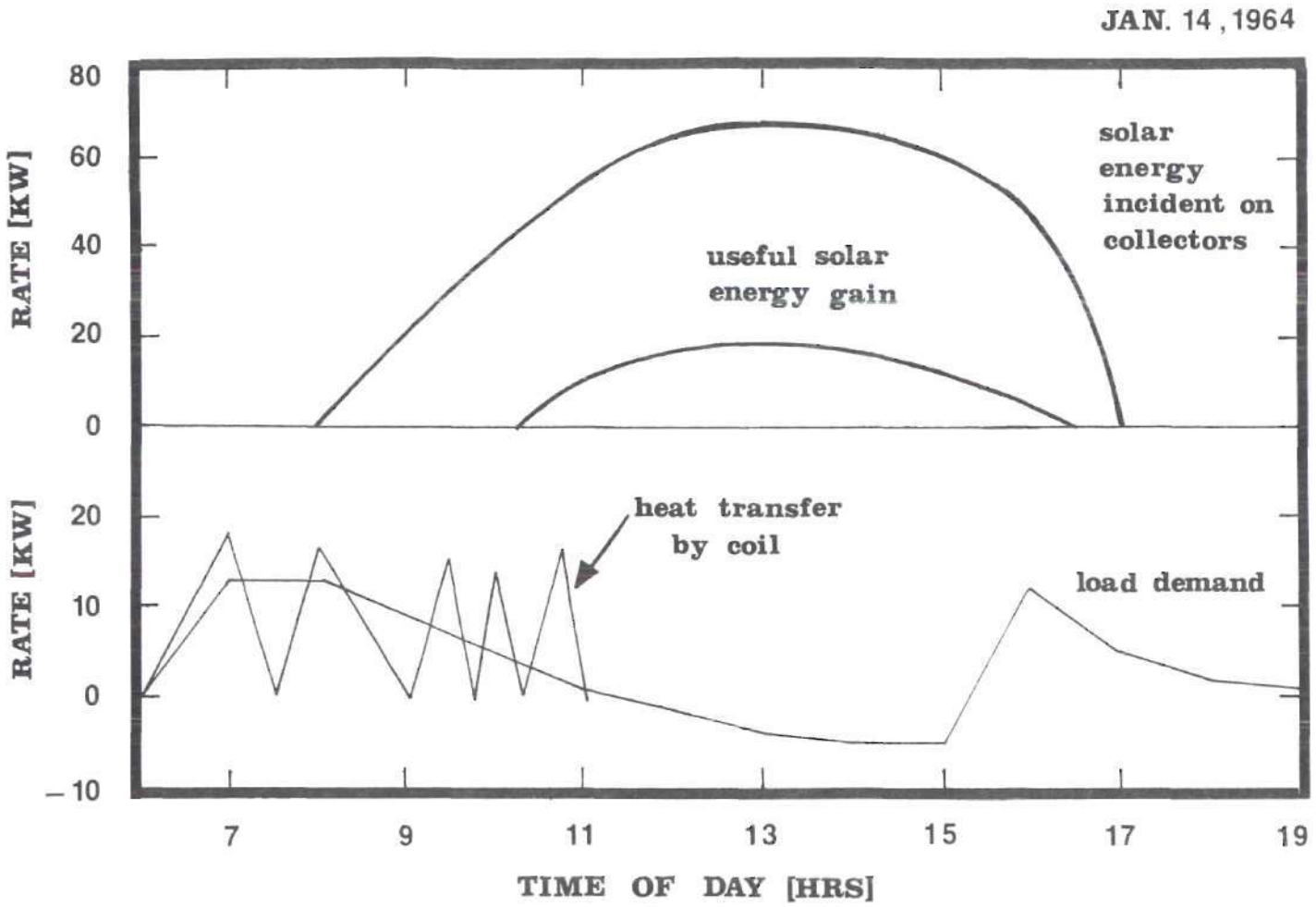

Figure 11b. Heat Transfer Rates: Heating

Date: January 14, 1964

TIME (HR)	MODE					
6-7	4333433343	3343343334	3334333433	3433433343	3343334333	4333433343
7-8	3433343334	3334333433	3433343334	3334333433	3433343334	3333433343
8-9	3343334333	4334333433	4334333433	4334334343	3433434334	3343433434
9-10	3433434343	4343433434	3434434343	4343443434	3443434434	4343443443
10-11	4434434443	4434443444	3444344434	4443444434	4442212222	2212222222
11-12	2212222222	2222222222	2222222222	2222222222	2222222222	2222222222
12-13	2222222222	2222222222	2222222222	2222222222	2222222222	2222222222
13-14	2222222222	2222222222	2222222222	2222222222	2222222222	2222222222
14-15	2222222222	2222222222	2222222222	2222222222	2222222222	2222222222
15-16	2222222222	2222222222	2222222222	2222222222	2222222222	2222222222
16-17	24444444444	4444444444	4444444444	4444444444	4444444444	4444444444
17-18	4444444444	4444444444	4444444444	4444444444	4444444444	4444444444
18-19	4444444444	4444444444	4444444444	4444444444	4444444444	4444444444

Figure 11c. Mode of Operation: Heating

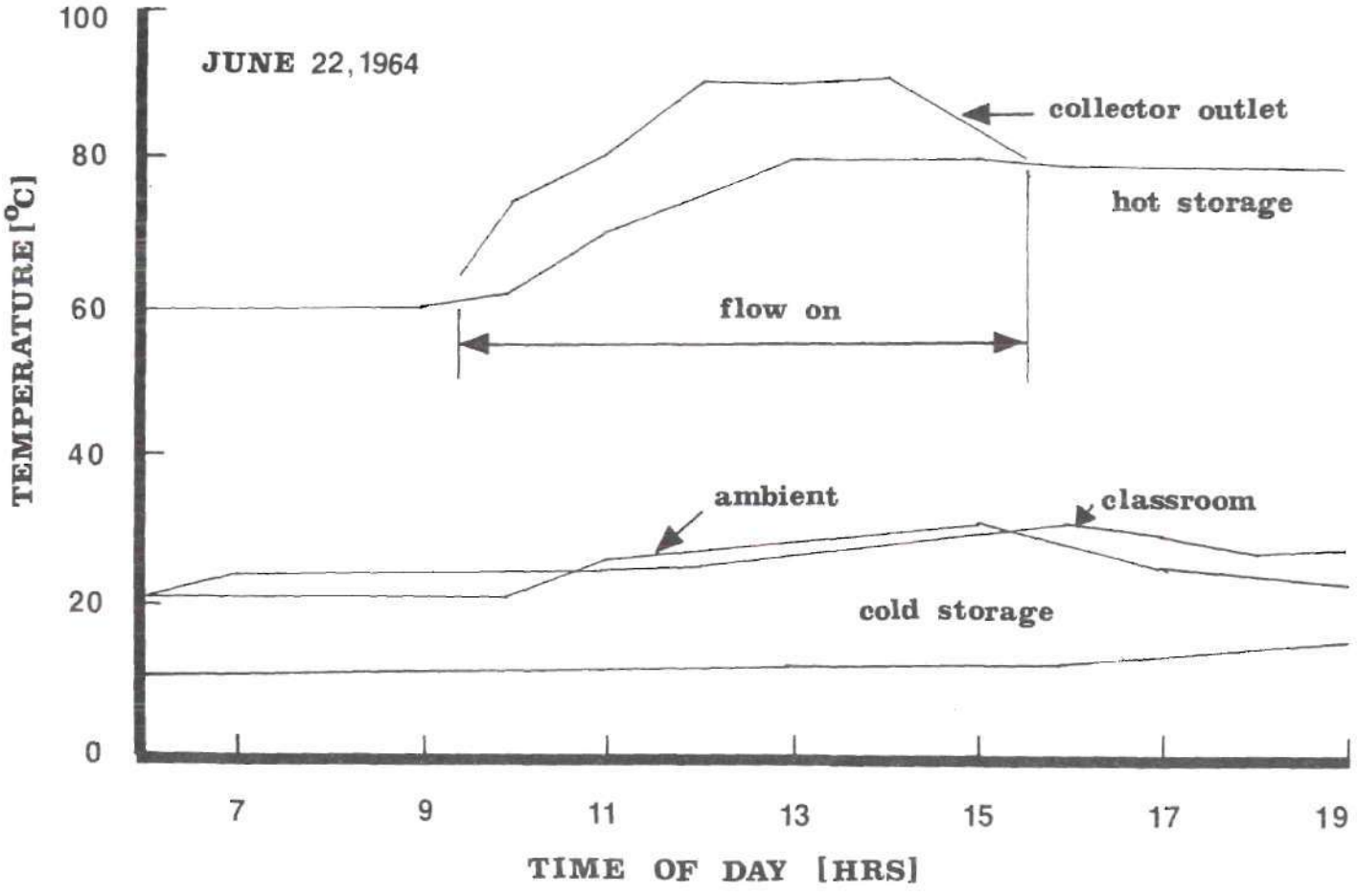

Figure 12a. Temperature Profiles: Cooling

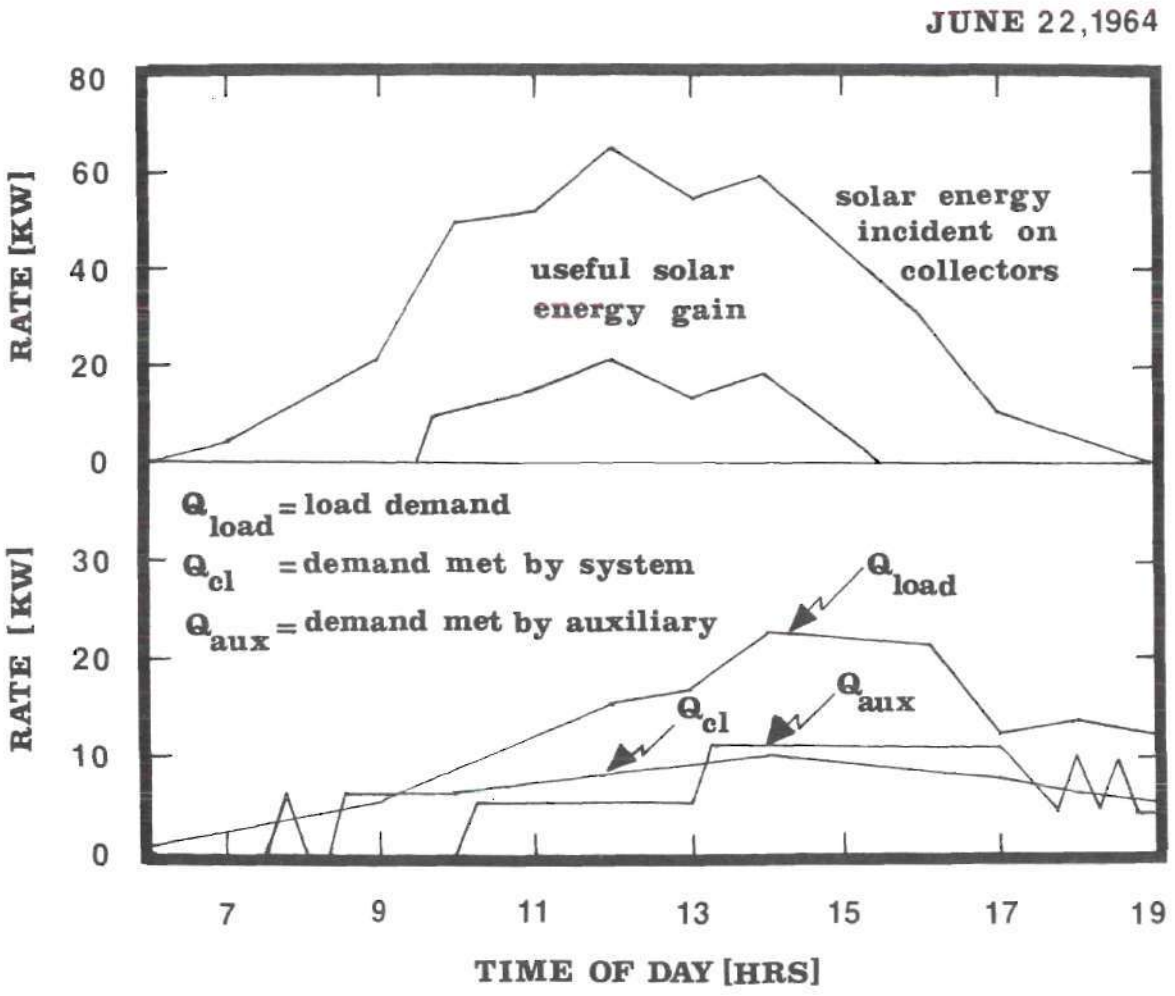

Figure 12b. Heat Transfer Rates: Cooling

Date: June 22, 1964

TIME(HR)	MODE					
6-7	7777777777	7777777777	7777777777	7777777777	7777777777	7777777777
7-8	7777777777	7777775775	7757757757	5775757757	5757575757	5757575757
8-9	5575757557	5575755755	7557557555	7557555755	5575555755	5575555555
9-10	7555555555	5555555555	5555555555	8888888888	8888888888	8888888888
10-11	8888888888	8888888888	8888888888	8888333333	3333333333	3333333333
11-12	3333333333	3333333333	3333333333	3333333333	3333333333	3333333333
12-13	3333333333	3333333333	3333333333	3333333333	3333333333	3333333333
13-14	3333333333	3333333333	3333333333	3333333333	3333333333	3333333333
14-15	3333333333	3333333333	3333333333	3333333333	3333333333	3333333333
15-16	3333333333	3333333333	3333333333	3344444444	4444444444	4555555555
16-17	5555555555	5555555555	5555555555	5555555555	5555555555	5555555555
17-18	5555555555	5555555555	5555555555	5555555555	5555555555	5555555555
18-19	5555555555	5555555555	5555555555	5555555555	5555555555	5555555555

Figure 12c. Mode of Operation: Cooling

for these days represent extreme combinations of the degree of sky cover and ambient air temperature. The meteorological data for these days are presented in Appendix D.

Hot Storage Capacity

The effects of hot storage capacity on collector efficiency are shown in Figures 13 and 14, respectively for the heating and cooling operation. For heating operation, the effect is most noticeable for April 15 which has a high value for the total daily solar radiation intensity. On such a day, much solar energy is collected and stored. A large storage capacity helps to reduce the storage water temperature and maintains a relatively low inlet fluid temperature to the collector. Consequently, energy loss from the collector to surroundings is reduced because the rate of energy loss is proportional to the collector fluid inlet temperature. The collector efficiency, therefore, increases.

On the other hand, a high inlet collector fluid temperature is desired for cooling operation to ensure a high collector outlet fluid temperature required by the absorption chiller for efficient operation. The cost for this manner of operation is a reduction in collector efficiency.

Collector Area

Reducing collector area increases collector efficiency. Less solar energy is collected and stored; consequently, a lower hot storage water temperature and therefore a lower collector inlet fluid temperature. Shown in Figures 15 and 16 are the effects of collector area for heating and cooling operation, respectively.

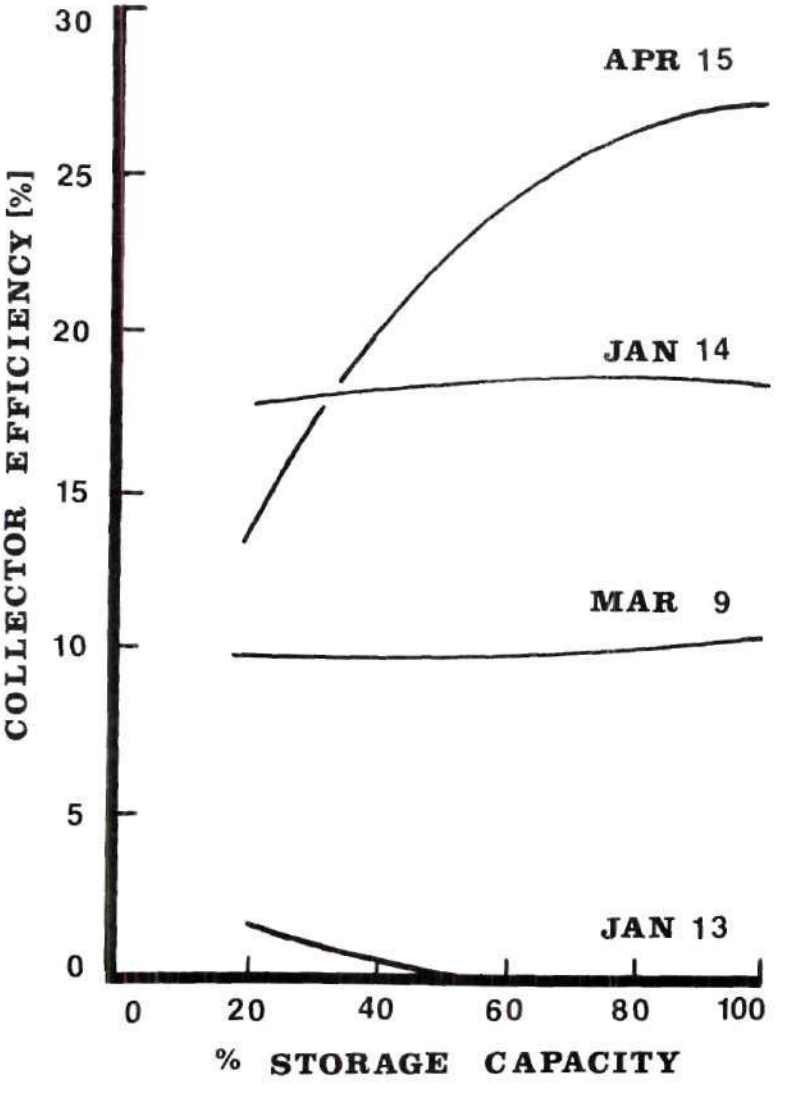

Figure 13. Effect of Hot Storage Capacity on Collector Efficiency: Heating

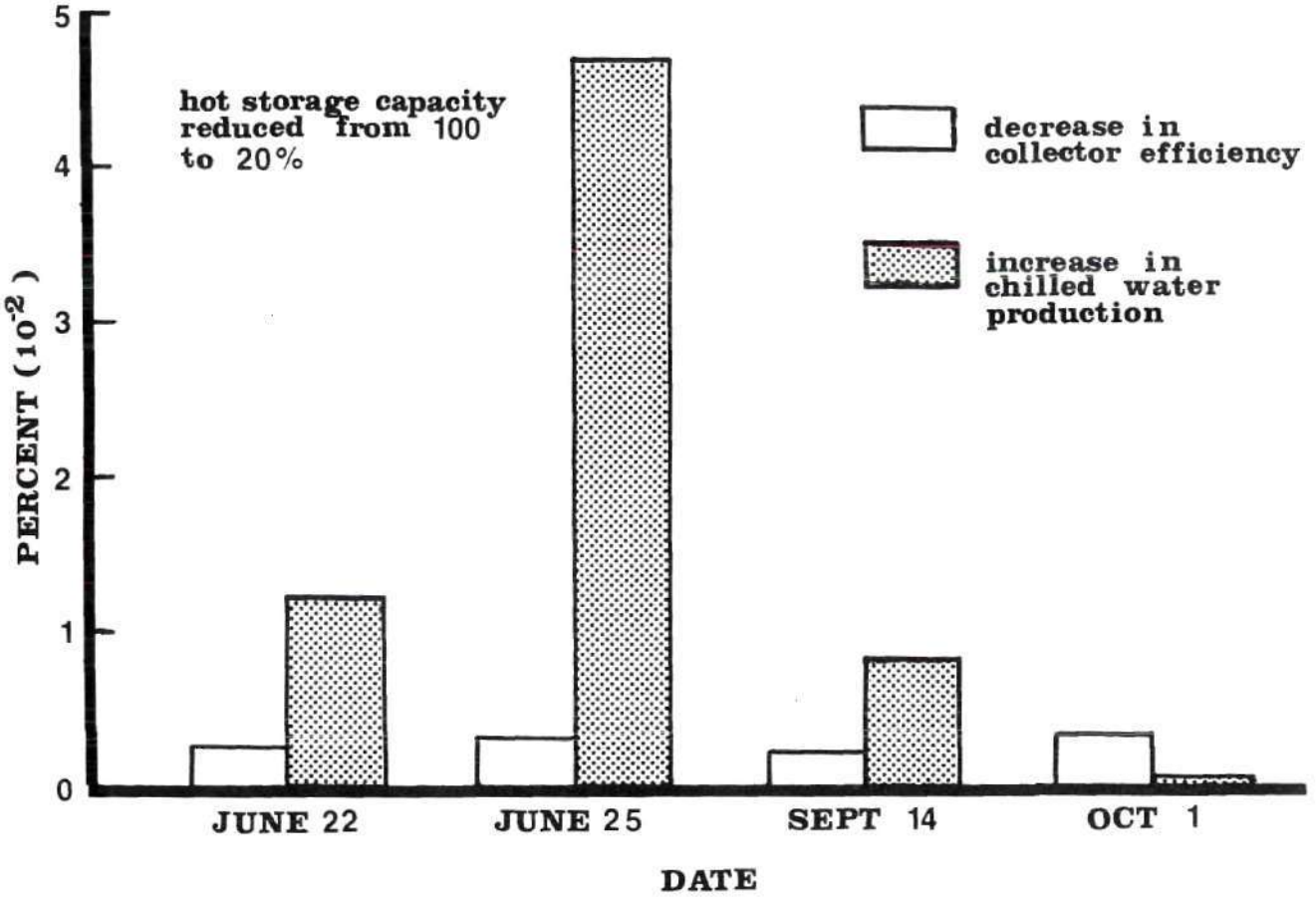

Figure 14. Effects of Hot Storage Capacity: Cooling

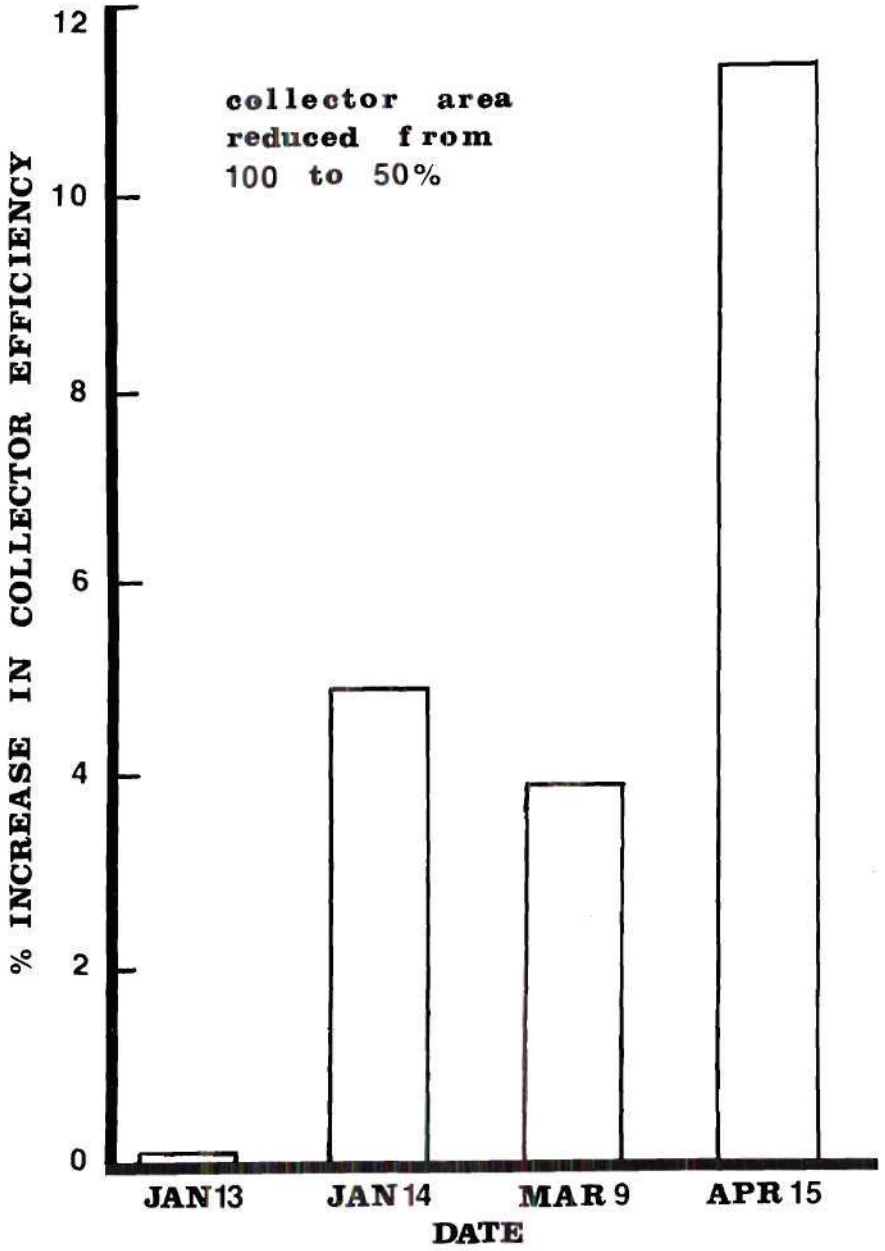

Figure 15. Effect of Collector Area on Collector Efficiency: Heating

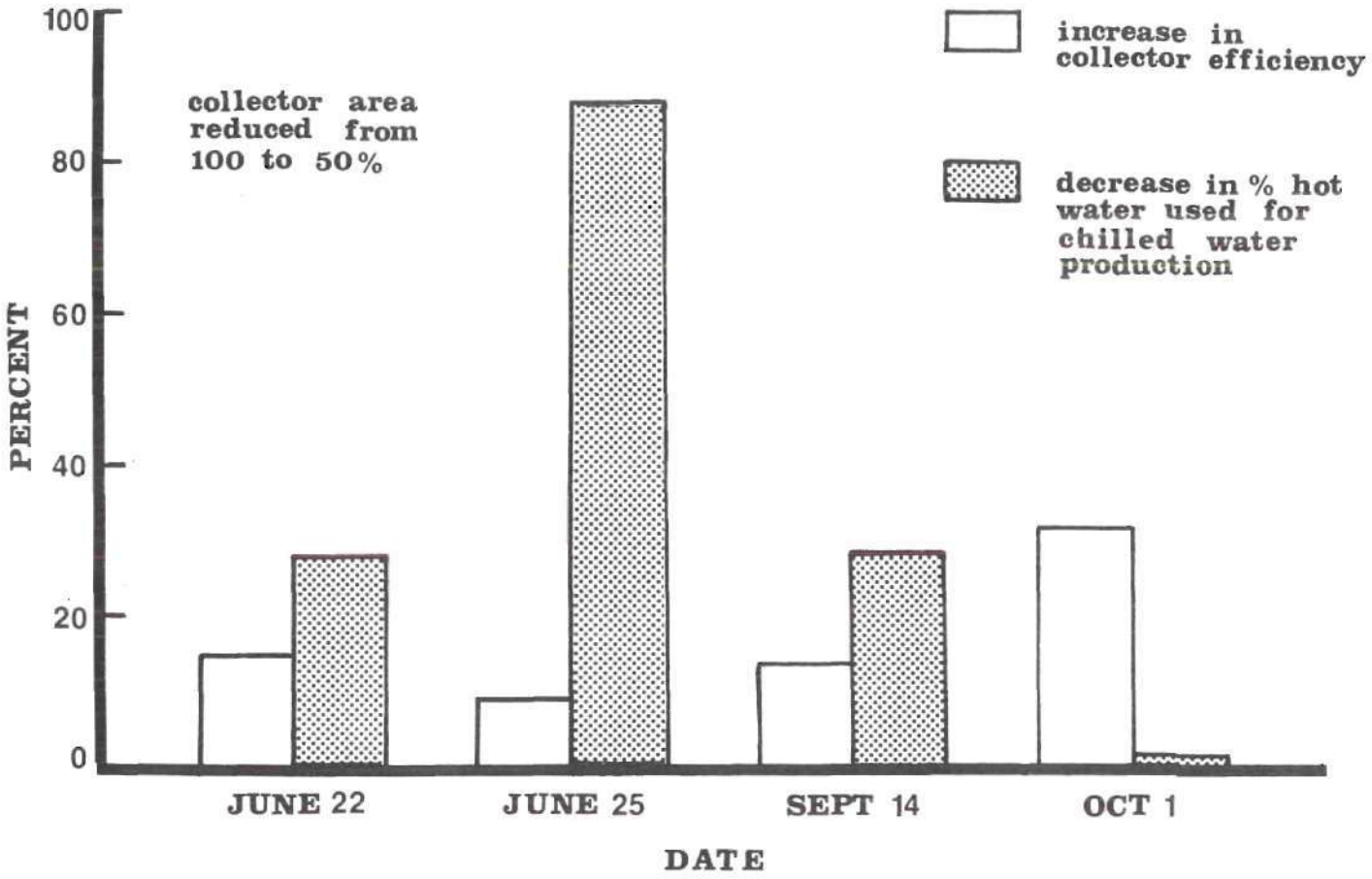

Figure 16. Effects of Collector Area: Cooling

Collector Fluid Flow Rate

High fluid flow rate through the collector produces a low outlet fluid temperature. As shown in Figure 18, this is undesirable for cooling operation because a lower percentage of the solar energy collected could be used for chilled water production.

For heating operation, the collector efficiency for a day with low total daily solar radiation value is not affected by the variation in collector fluid flow rate. On the other hand, when the total daily radiation value is high, the collector efficiency decreases with a reduction in fluid flow rate resulting from the many shutdowns of the collector system due to high fluid outlet temperature, near the boiling point. Figure 17 shows the effect of this parameter.

Collector Loss Coefficient

Reducing the collector loss coefficient by means of selective coatings or increasing the number of glass covers increases the collector efficiency. The effects of collector loss coefficient on collector efficiency are shown in Figures 19 and 20.

Differential Temperature Between Hot Storage and Collector

For heating operation, Figure 21 shows that reducing the differential temperature between the hot storage and collector, required to initiate flow through the collector, increases the collector efficiency.

For cooling operation, no significant effect on collector efficiency was observed when the differential control temperature is increased on days with high total daily radiation. For days with low total daily radiation, collector efficiency decreases with increased differential

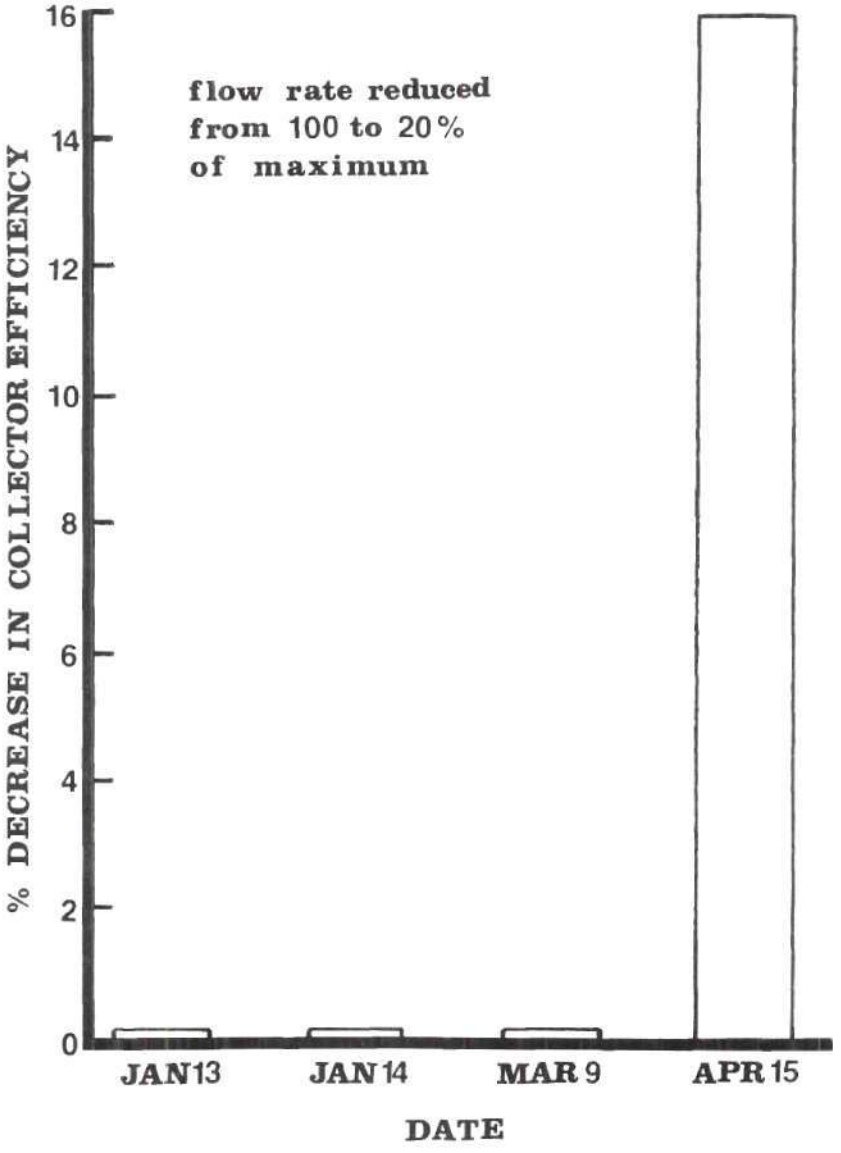

Figure 17. Effect of Collector Fluid Flow Rate on Collector Efficiency: Heating

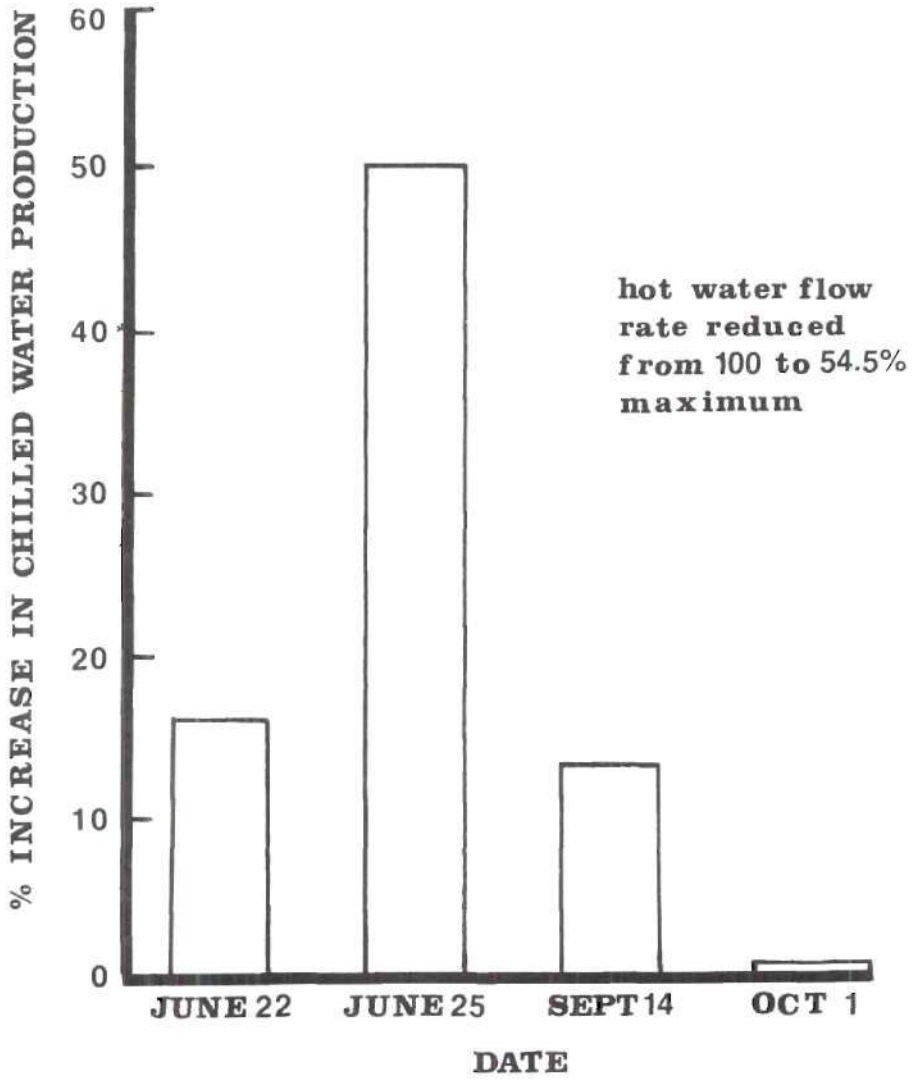

Figure 18. Effect of Increasing Hot Water Flow Rate on Chilled Water Production: Cooling

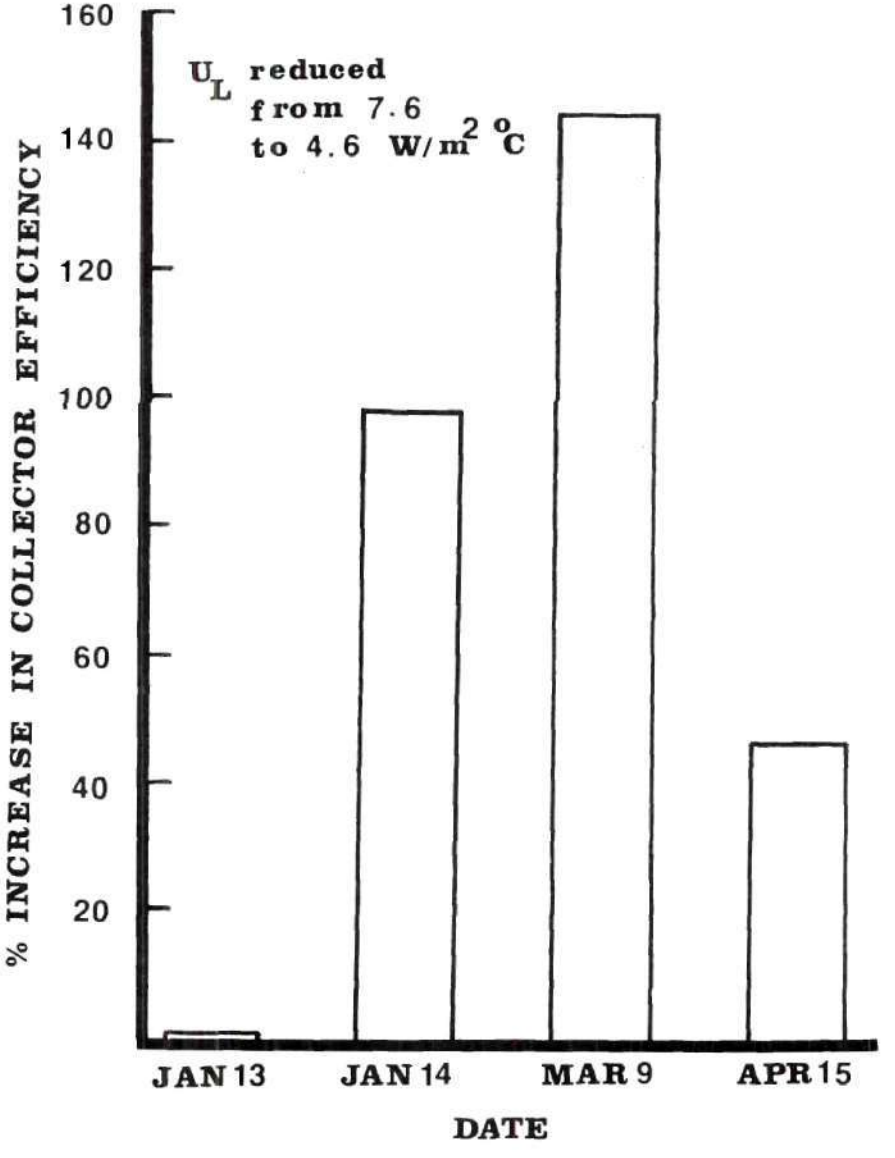

Figure 19. Effect of Collector Loss Coefficient on Collector Efficiency: Heating

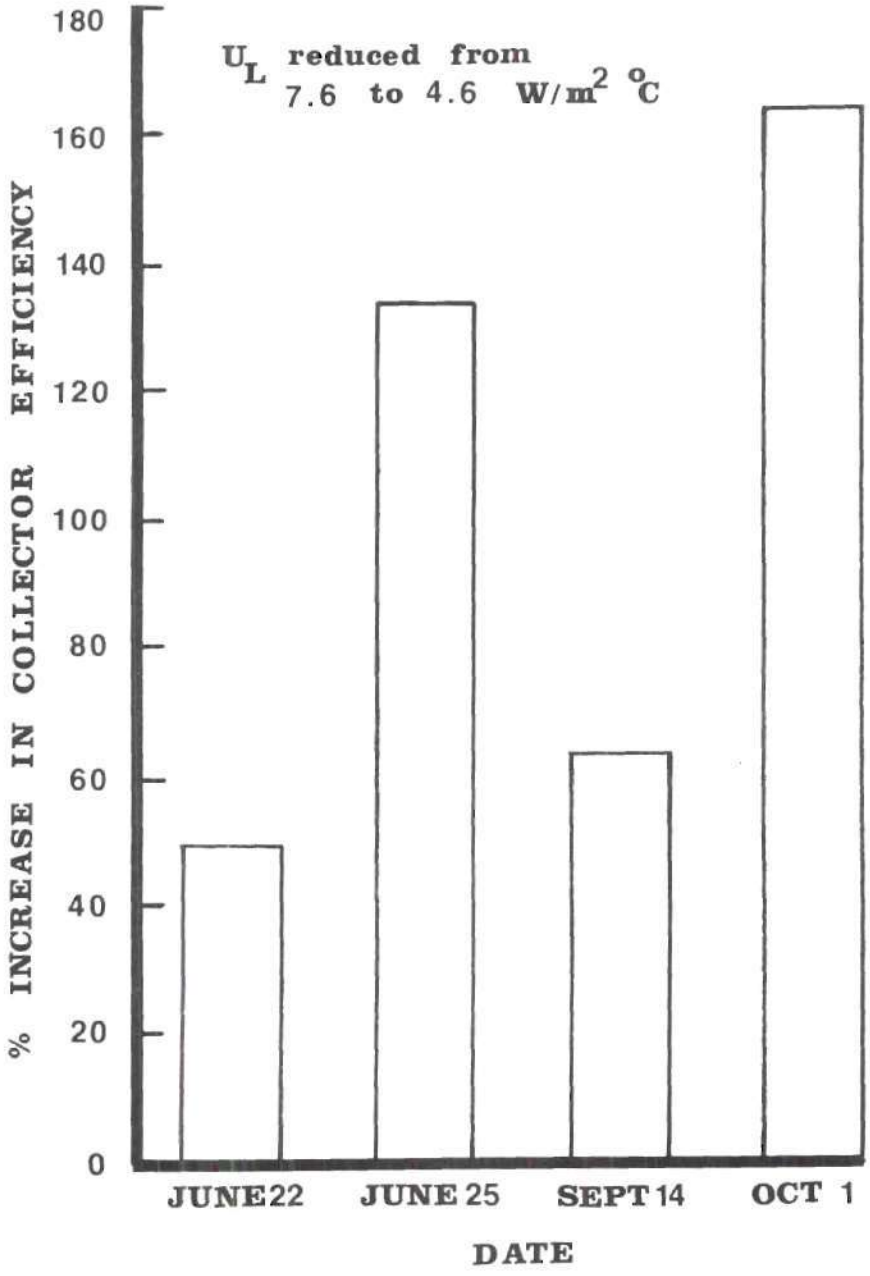

Figure 20. Effect of Collector Loss Coefficient on Collector Efficiency: Cooling

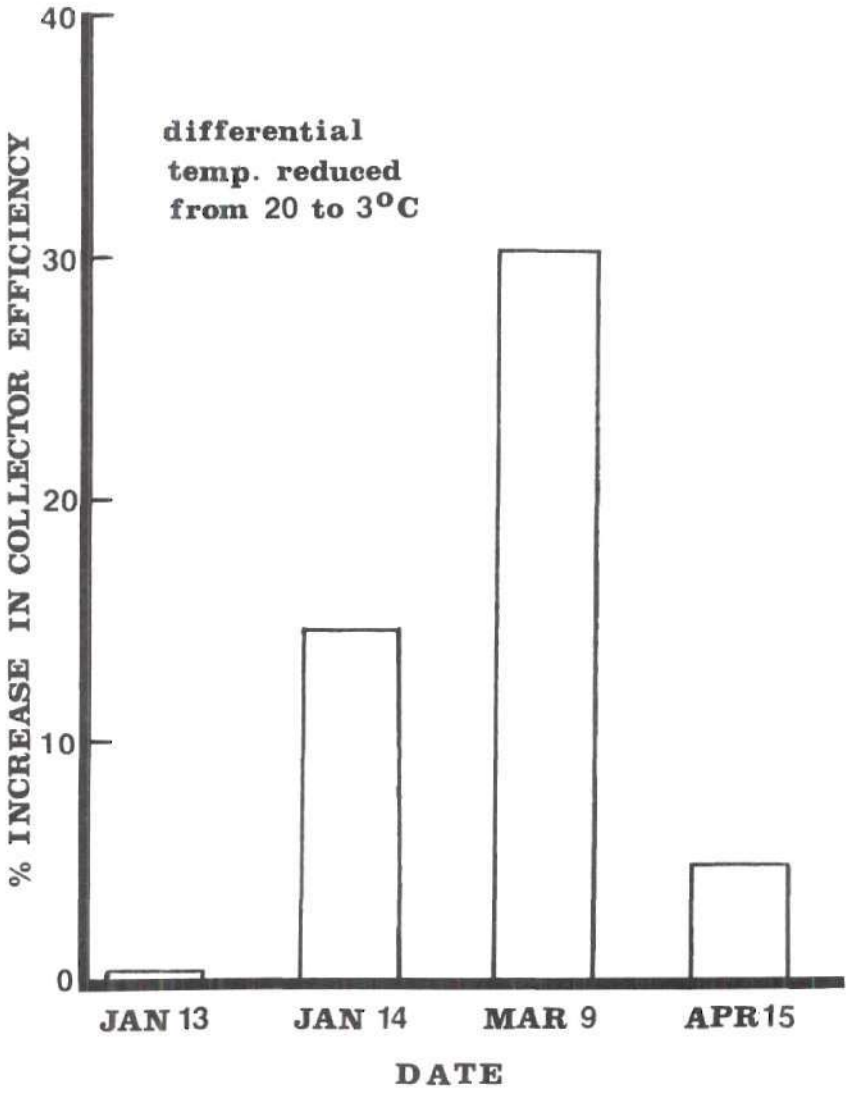

Figure 21. Effect of Differential Control Temperature Between Collector and Hot Storage on Collector Efficiency: Heating

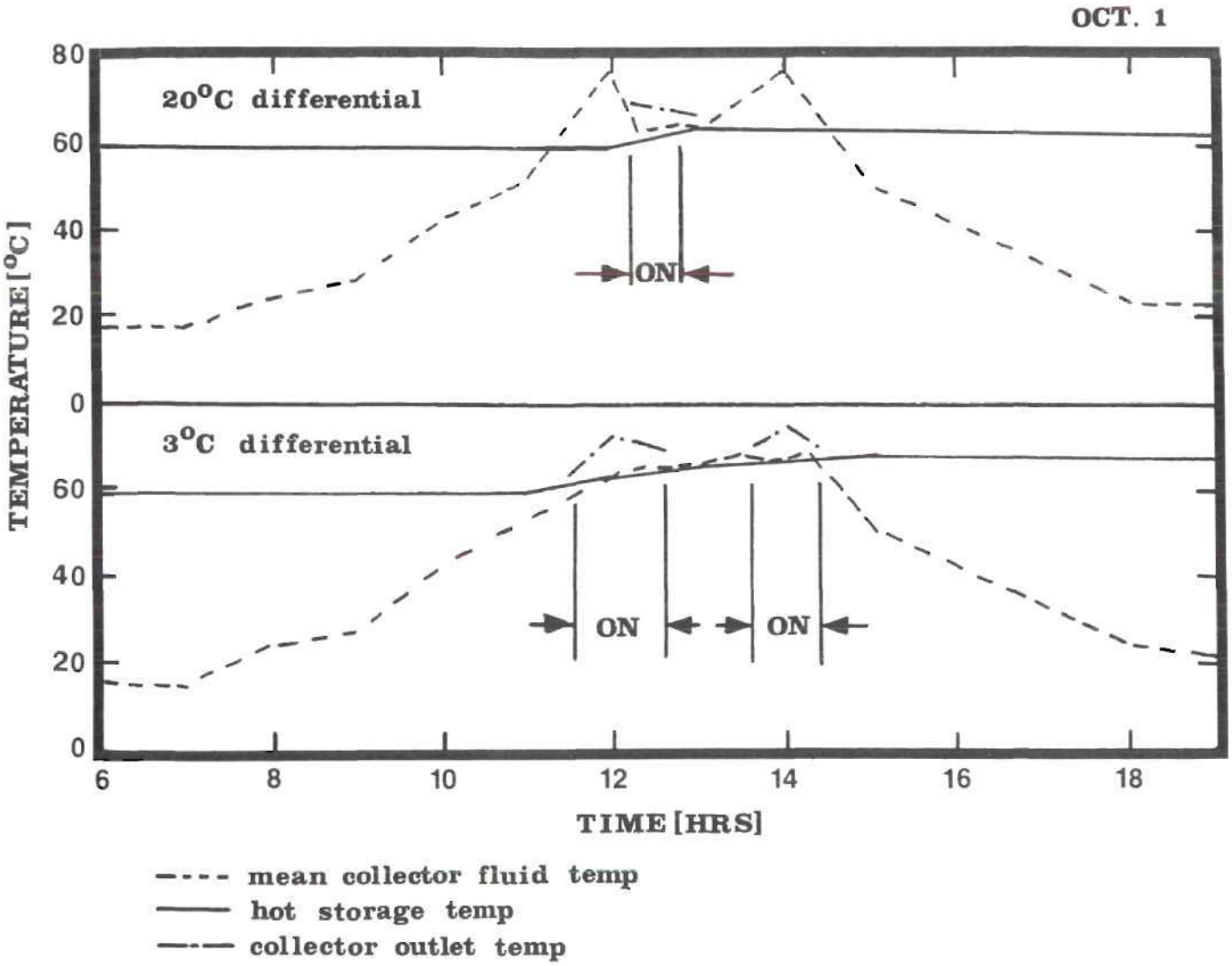

Figure 22. Effects of Differential Control Temperature Between Collector and Hot Storage: Cooling

control temperature. Figure 22 shows this effect on component temperature profiles.

Therefore, a low differential control temperature between hot storage and collector is a highly desirable feature for both heating and cooling operations.

Chilled Water Storage Capacity

The use of chilled water storage in conjunction with lithium bromide absorption chiller allows improved operating conditions of the cooling subsystem. Significant performance degradation in absorption cooling capacity is evident whenever the chiller cycles on and off during periods of low cooling demand. The capability of providing large storage for the chiller output prevents short-term cycling of the absorption machine and improves the performance of the cooling subsystem.

Parameters Produced No Significant Effects

Varying the chilled water flow rate and the set temperature of the classroom interior have no effect on system performance. Increasing the set temperature for the classroom did, however, decrease the auxiliary cooling requirement.

System Simulation

The solar system was simulated for two months of the year: January and June of 1964. System performances for January and June are shown in Figures 23 and 24, respectively.

The system meets 100% of the heating load demand and approximately 32% of the cooling load. The average monthly collector efficiencies for

January and June are approximately the same, 20%. The average monthly Cop for the chiller is 0.7.

The amount of useful solar energy collected could be increased by lowering the slope of the collector array from 45^{o} to 23^{o} from the horizontal as shown in Figure 25. However, to take full advantage of this increase in solar energy collected, the design delivered capacity of the absorption chiller would have to be increased. Otherwise, the flow rate to the collector and the hot storage capacity must be increased to prevent boiling of the collector fluid because of the added useful solar energy, and subsequent collector system shutdown.

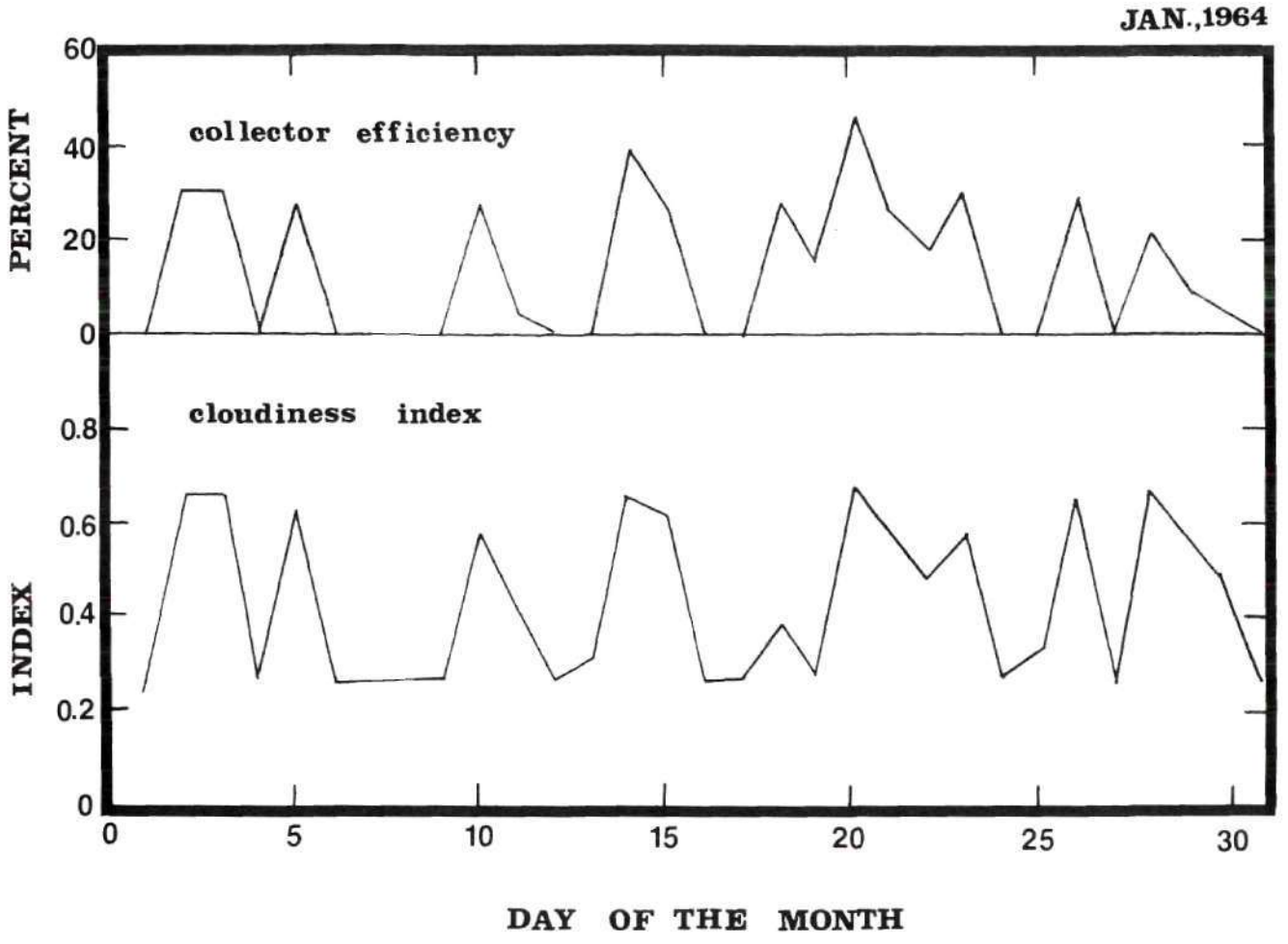

Figure 23. System Performance for January 1964

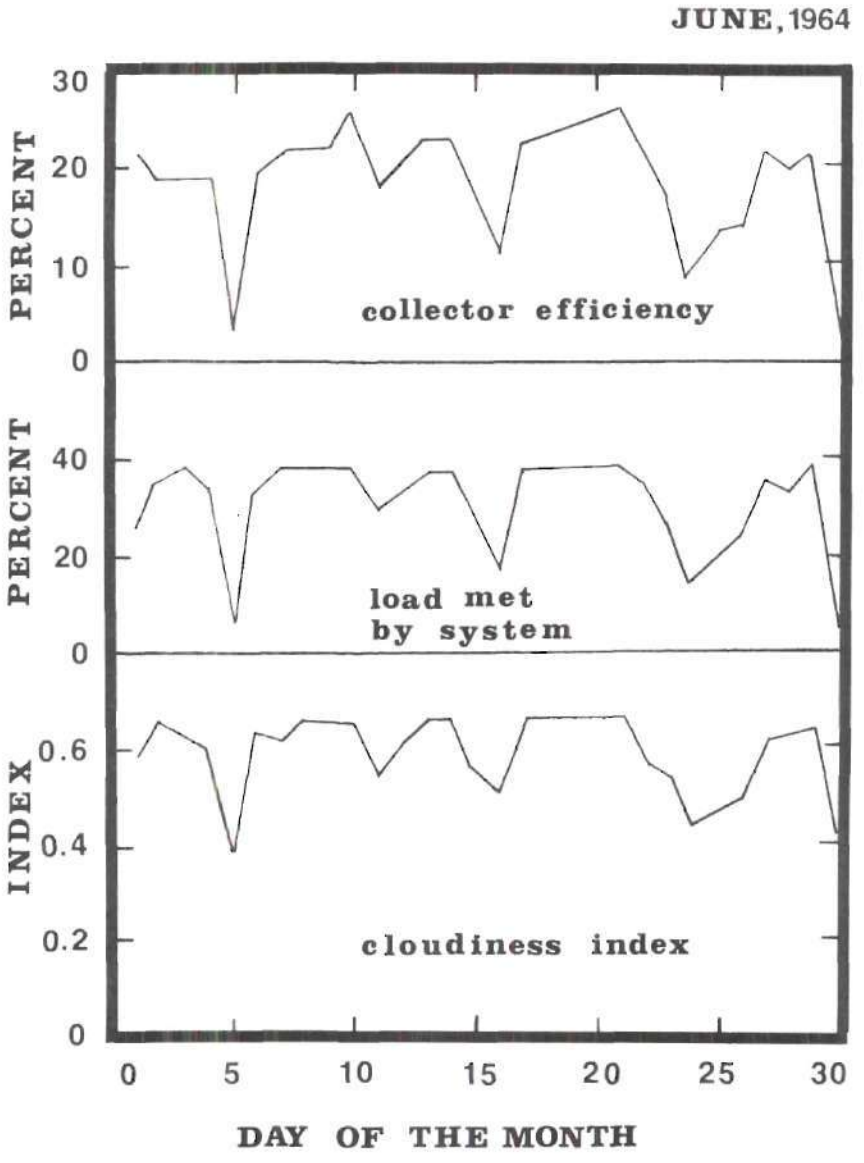

Figure 24. System Performance for June 1964

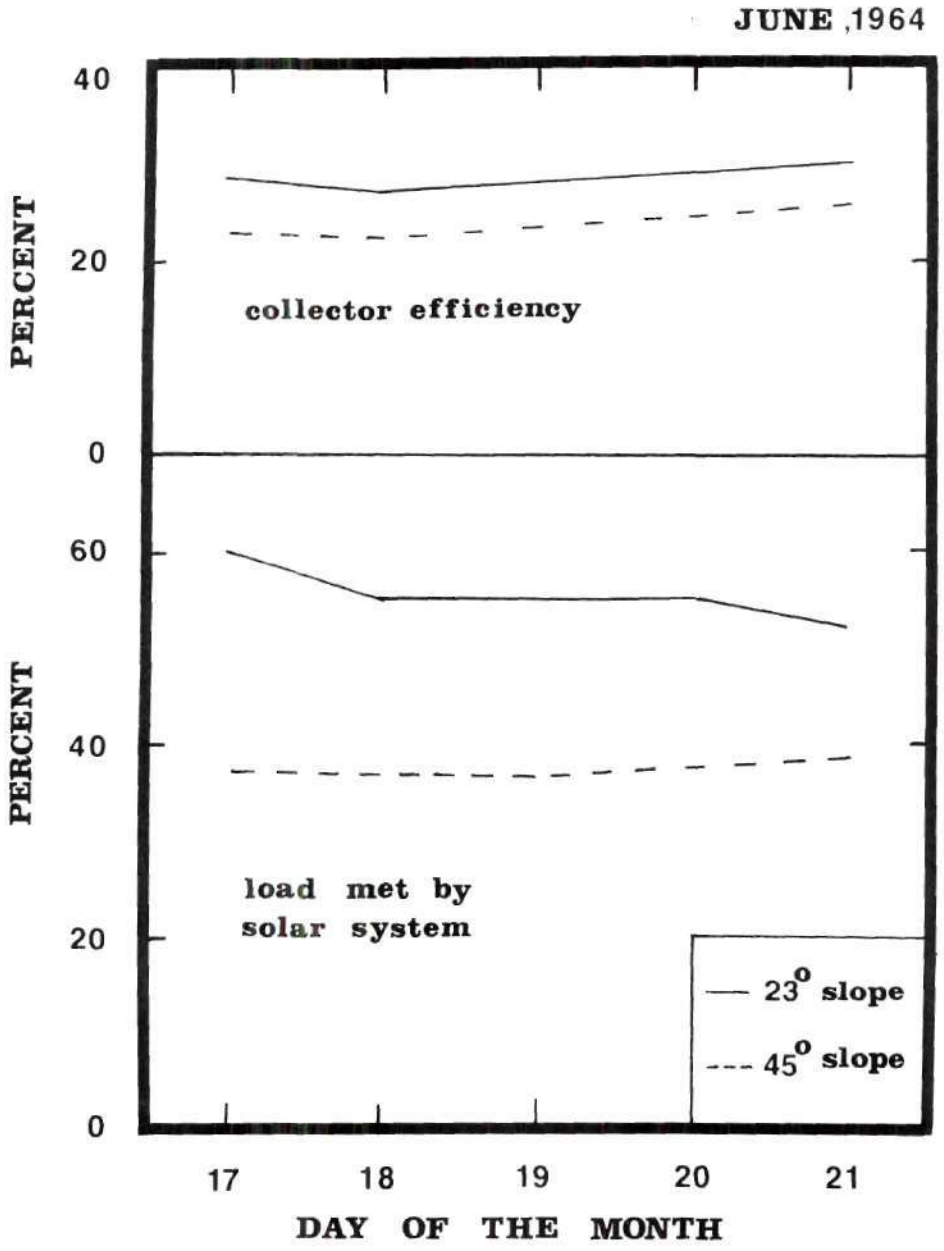

Figure 25. Effects of Changing Collector Slope: Cooling

CHAPTER VII

CONCLUSIONS AND RECOMMENDATIONS

Conclusions

The control strategies that would operate the multi-mode solar system of Georgia Tech in an optimized manner are as follows:

For heating operation,

1. use maximum hot storage capacity,
2. operate the system with a minimum total collector area, necessary to collect the required solar energy to meet heating load demand,
3. operate with maximum fluid flow rate through the collector array, and
4. a low differential control temperature between the hot storage and collector to initiate flow through the collector array.

For cooling operation,

1. use minimum hot storage capacity and maximum chilled water storage capacity,
2. use maximum total collector area,
3. operate with a low fluid flow rate through the collector array; the minimum value is governed by the required design flow rate for the absorption chiller, and
4. operate with a low differential control temperature

between the hot storage and collector to initiate flow to the collector array.

Recommendations

Recommendations for future development and upgrading of the multi-mode solar system computer simulation program are as follows:

1. provide program flexibility to enable the simulation of a general multi-mode solar system, and
2. upgrade the storage tank component model to one which includes thermal stratification.

APPENDICES

APPENDIX A

THERMAL CAPACITANCE CALCULATIONS OF ISOTHERMAL SECTIONS

Exterior Walls

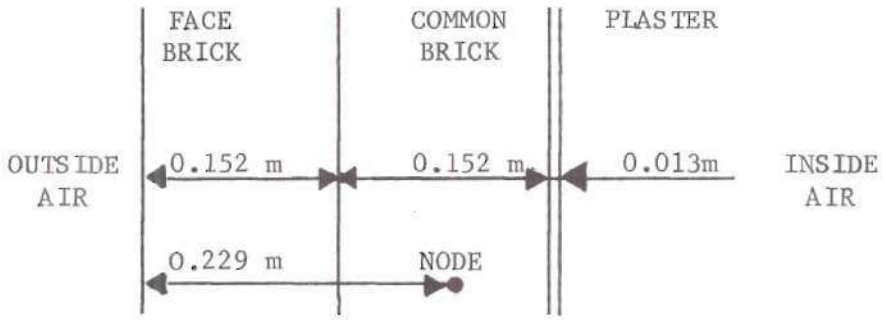

Surface conductance is given by the equation (3):

$$f = 11.4 + 4.4\,W \qquad \text{(A-1)}$$

where f = surface conductance, $W/m^{2}{}^{o}C$

W = wind speed, m/s

Average total resistance for the wall is

		Resistance $\left(\frac{m^{2}{}^{o}C}{W}\right)$
1.	Outside surface (W = 5m/s)	0.03
2.	Face brick	0.12
3.	Common brick	0.21
4.	Plaster	0.02
5.	Inside air	0.12
		0.50

Therefore, the node is to be located 0.229 m from the outside surface.

The thermal conductance between the node and the exterior is

$$C_{o} = \frac{1}{\frac{1}{f} + 0.22} \qquad \text{(A-2)}$$

where C_o = thermal conductance between the node and exterior, $W/m^{2o}C$

The thermal conductance between the node and the interior is

$$C_i = 4.1\ W/m^{2o}C$$

The effective thermal capacitance of the wall is given by

$$M_W C_W = (\text{density x specific heat x length})_W \qquad \text{(A-3)}$$

For face brick + common brick

$$M_W C_W = 2000\ \frac{kg}{m^3} \times 0.84\ \frac{kJ}{kg\ ^oC} \times 0.304\ m$$

$$= 510.7\ \frac{kJ}{m^{2o}C}$$

For plaster

$$M_W C_W = 1799\ \frac{kg}{m^3} \times 0.92\ \frac{kJ}{kg\ ^oC} \times 0.013\ m$$

$$= 20.5\ \frac{kJ}{m^{2o}C}$$

Total $M_w C_w = 531\ \frac{kJ}{m^{2o}C}$

Roof

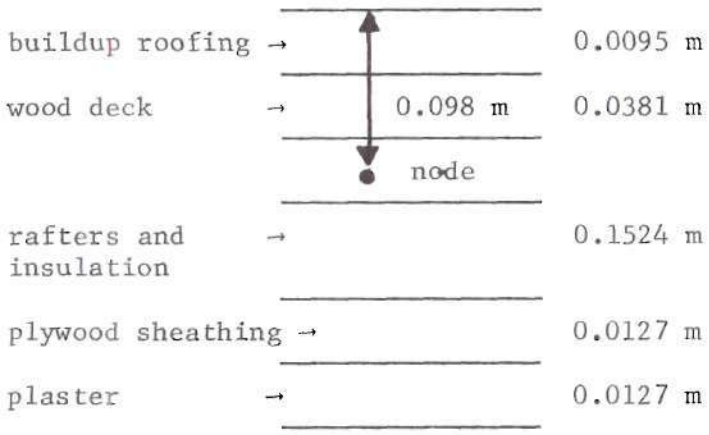

Average total resistance

	Resistance $\left(\frac{m^{2o}C}{W}\right)$
1. Outside air (W = 5m/s)	0.03
2. Buildup roofing	0.06
3. Wood deck	0.33
4. Roof insulation and rafters	1.20
5. Plywood sheathing	0.11
6. Plaster	0.02
7. Inside air	0.11
	1.86

Therefore, the node is located approximately 0.098m from the outside surface. Thermal conductance between the node and interior is

$$C_i = 0.97 \ W/m^{2o}C$$

and the thermal conductance between the node and the exterior is

$$C_o = \frac{1}{\frac{1}{f} + 0.79} \ W/m^{2o}C$$

Effective thermal capacitance is

Buildup roofing

$$MC = 1121 \frac{kg}{m^3} \times 1.47 \frac{kJ}{kg\,^oC} \times 0.0095\ m$$

$$= 15.6 \frac{kJ}{m^2\,^oC}$$

Plywood deck

$$MC = 699.7 \frac{kg}{m^3} \times 2.09 \frac{kJ}{kg\,^oC} \times 0.0381\ m$$

$$= 55.7 \frac{kJ}{m^2\,^oC}$$

Rafters and insulation (assume 15% of volume is frame)

frame

$$MC = 699.7 \frac{kg}{m^3} \times 2.09 \frac{kJ}{kg\,^oC} \times 0.1525\ m \times 0.15$$

$$= 33.4 \frac{kJ}{m^2\,^oC}$$

insulation

$$MC = 99.9 \frac{kg}{m^3} \times 0.84 \frac{kJ}{kg\,^oC} \times 0.1524\ m \times 0.85$$

$$= 10.8 \frac{kJ}{m^2\,^oC}$$

Plywood and sheathing

$$MC = 599.7 \frac{kg}{m^3} \times 2.5 \frac{kJ}{kg\,^oC} \times 0.0127\ m$$

$$= 19.0 \ \frac{kJ}{m^2 {}^oC}$$

plaster

$$MC = 1799 \ \frac{kg}{m^3} \times 0.92 \ \frac{kJ}{kg \ {}^oC} \times 0.0127 \ m$$

$$= 21 \ \frac{kJ}{m^2 {}^oC}$$

$$\text{Total} = 156 \ \frac{kJ}{m^2 {}^oC}$$

APPENDIX B

FAN COIL PERFORMANCE DATA, DERIVATION OF THE SENSIBLE TO TOTAL HEAT TRANSFER RATIO, R_Q

Table 3. Fan-Coil Performance Data

Run	AIR				WATER		HEAT TRANSFERRED	
	Enter		Exit		Enter	Exit	Total	Sensible
	T_d (°F)	T_w (°F)	T_d (°F)	T_w (°F)	°F	°F	Btu/h	Btu/h
1	80	70	59.0	56.5	42	53.9	53595	27468
2	80	67	58.0	54.8	42	52.2	45715	28711
3	80	64	56.2	52.7	42	50.9	40235	30476
4	80	67	59.3	56.1	45	54.2	41390	27010
5	80	64	58.0	54.0	45	53.0	36000	28776
6	80	67	60.9	57.7	48	56.0	36000	24917
7	80	64	59.3	55.3	48	55.0	31700	27076

Derivation of Equation 3.15 (Equation for R_Q)

The sensible heat removed by the fan-coil unit when in cooling operation is given by

$$Q_S = 1.02\ (T_{di} - T_{do}) \qquad \text{(B-1)}$$

where Q_S = sensible heat removed, kJ/kg of dry air

T_{di} = inlet dry-bulb air temperature, ^oC

T_{do} = outlet dry-bulb air temperature, ^oC

The enthalpy of air is found by adding the enthalpy per kg of dry air and the enthalpy of the water vapor (steam) associated with the kg of dry air. The resulting equation is of the form:

$$h_a = T_d + S_i(2500 + 1.86\ T_d) \qquad \text{(B-2)}$$

where h_a = enthalpy of air, kJ/kg of dry air

T_d = dry-bulb air temperature, ^oC

S_i = inlet air specific humidity, kg of steam per kg of dry air

The amount of total heat removed in the fan-coil is given by

$$Q_T = (h_a)_i - (h_a)_o \qquad \text{(B-3)}$$

where Q_T = total heat removed, kJ/kg of dry air

$(h_a)_i$ = enthalpy of inlet air, kJ/kg of dry air

$(h_a)_o$ = enthalpy of outlet air, kJ/kg of dry air

Substituting equation B-2 into equation B-3 and rearranging, the equation becomes

$$Q_T = (1 + 1.86\ S_i)\ (T_{di} - T_{do}) + (-0.0048179 + 0.0046635\ R_Q)(2500 + 1.86\ T_{do}) \quad \text{(B-4)}$$

where S_i = inlet air specific humidity, kg of steam/kg of dry air

T_{di} = inlet dry-bulb air temperature, ^oC

T_{do} = outlet dry-bulb air temperature, ^oC

R_Q = ratio of sensible to total heat removed, dimensionless

The ratio of sensible to total heat removed is given by

$$R_Q = \frac{Q_S}{Q_T} \quad \text{(B-5)}$$

$$= \frac{1.02(T_{di} - T_{do})}{\left\{(1 + 1.86S_i)(T_{di} - T_{do}) + (-0.0048179 + 0.0046635R_Q)(2500 + 1.86T_{do})\right\}}$$

Rearranging

$$R_Q = \frac{-(\alpha + a\beta) + \sqrt{(\alpha + a\beta)^2 + 4b\beta\gamma}}{2b\beta} \quad \text{(B-6)}$$

where $\alpha = (1 + 1.86S_i)(T_{di} - T_{do})$

$\beta = (2500 + 1.86T_{do})$

$\gamma = 1.02(T_{di} - T_{do})$

$a = -0.0048179$

$b = 0.0046635$

APPENDIX C

ABSORPTION CHILLER PERFORMANCE DATA

Table 4. Absorption Chiller Performance Data

Hot Water		Energy Input	Delivered Capacity	
Inlet	Outlet	Btu/h	Btu/h	Tons
170°F	167.4	14.500	6.400	0.53
175°F	171.1	21.600	13.100	1.09
180°F	174.8	28.800	19.400	1.62
185°F	178.5	35.900	25.600	2.13
190°F	182.2	42.900	31.300	2.61
195°F	185.9	50.000	36.000	3.00
200°F	189.8	56.000	40.200	3.35
205°F	193.9	60.800	42.000	3.50

Inlet Condensing Water Temperature = 85°F

APPENDIX D

METEOROLOGICAL DATA FOR EIGHT SELECTED DAYS IN 1964 FOR ATLANTA

Table 5a. Meteorological Data for Eight Selected Days

Date: 13/1/1964

Time (h)	Solar Rad. on Hor. Surf (W/m^2)	Wind Speed (m/s)	Temp. (^oC)	Rel. Humid (%)
6	0.0	7.71	- 3.33	78.0
7	0.0	5.65	- 3.89	75.0
8	.5	7.20	- 3.33	75.0
9	43.6	6.68	- 3.33	85.0
10	169.6	8.74	- 3.89	88.0
11	131.9	6.68	- 6.11	78.0
12	281.2	8.74	- 5.56	65.0
13	208.1	9.25	- 5.56	65.0
14	329.1	8.22	- 6.11	74.0
15	154.0	8.74	- 5.56	68.0
16	220.2	7.71	- 6.11	68.0
17	42.5	7.71	- 6.11	71.0
18	0.0	7.71	- 6.67	68.0
19	0.0	6.17	- 7.22	71.0

Table 5b: Meteorological Data for Eight Selected Days

Date: 14/1/1964

Time (h)	Solar Rad. on Hor. Surf (W/m^2)	Wind Speed (m/s)	Temp. (^oC)	Rel. Humid (%)
6	0.0	5.14	- 8.33	71.0
7	0.0	4.11	- 8.33	74.0
8	1.2	5.65	- 8.89	77.0
9	162.6	8.74	- 9.44	74.0
10	347.7	8.22	- 8.33	62.0
11	490.8	6.68	- 6.67	57.0
12	576.6	5.14	- 5.56	51.0
13	597.5	5.14	- 2.78	45.0
14	552.0	5.65	- 1.67	45.0
15	443.6	3.60	- .56	41.0
16	282.5	4.11	0.00	42.0
17	90.0	4.63	.56	43.0
18	0.0	3.60	0.00	43.0
19	0.0	4.63	- 1.11	49.0

Table 5c: Meteorological Data for Eight Selected Days

Date: 9/3/1964

Time (h)	Solar Rad. on Hor. Surf (W/m^2)	Wind Speed (m/s)	Temp. (^oC)	Rel. Humid (%)
6	0.0	4.11	8.33	97.0
7	0.0	4.11	7.22	100.0
8	69.7	3.60	6.67	100.0
9	100.5	5.14	6.11	93.0
10	282.1	6.68	5.56	81.0
11	197.2	7.71	6.67	78.0
12	609.8	6.17	7.22	73.0
13	670.4	6.17	9.44	63.0
14	593.6	6.68	8.89	59.0
15	185.9	7.71	7.22	61.0
16	253.3	7.20	7.78	59.0
17	81.6	7.20	8.33	64.0
18	36.0	7.71	7.78	68.0
19	0.0	0.0	6.17	76.0

Table 5d: Meteorological Data for Eight Selected Days

Date: 15/4/1964

Time (h)	Solar Rad. on Hor. Surf (W/m^2)	Wind Speed (m/s)	Temp. (^oC)	Rel. Humid (%)
6	0.0	3.60	10.00	96.0
7	89.7	3.08	10.00	93.0
8	319.4	2.57	10.00	67.0
9	543.6	3.60	13.33	52.0
10	734.2	5.14	16.11	46.0
11	874.7	4.63	18.89	33.0
12	953.7	5.65	20.00	32.0
13	964.9	5.65	21.11	32.0
14	907.4	4.11	21.67	28.0
15	785.9	5.14	22.78	27.0
16	610.0	6.68	23.89	26.0
17	394.5	6.17	23.89	25.0
18	161.5	5.14	23.89	22.0
19	0.0	4.11	22.78	25.0

Table 5e: Meteorological Data for Eight Selected Days

Date: 22/6/1964

Time (h)	Solar Rad. on Hor. Surf (W/m^2)	Wind Speed (m/s)	Temp. (^oC)	Rel. Humid (%)
6	7.3	1.54	22.22	82.0
7	53.2	2.57	22.22	76.0
8	249.3	2.57	22.22	69.0
9	361.2	2.06	22.78	65.0
10	799.2	1.54	24.44	63.0
11	818.6	1.54	27.22	52.0
12	1005.0	2.57	27.22	49.0
13	895.5	2.57	28.89	41.0
14	957.2	2.57	31.11	43.0
15	711.3	1.54	31.67	36.0
16	585.4	1.54	28.89	31.0
17	135.0	6.17	24.44	45.0
18	138.6	4.11	23.89	47.0
19	20.1	4.11	23.33	59.0

Table 5f: Meteorological Data for Eight Selected Days

Date: 25/6/1964

Time (h)	Solar Rad. on Hor. Surf (W/m^2)	Wind Speed (m/s)	Temp. (^oC)	Rel. Humid (%)
6	6.7	1.54	21.67	84.0
7	52.5	2.06	21.67	90.0
8	202.3	3.08	21.67	82.0
9	167.5	3.60	22.22	79.0
10	589.9	2.57	22.22	79.0
11	427.2	3.08	23.33	77.0
12	843.4	4.11	25.00	77.0
13	803.6	3.08	27.22	77.0
14	870.4	3.08	28.33	72.0
15	523.3	3.08	24.44	63.0
16	691.2	4.63	27.78	65.0
17	135.4	3.60	26.67	84.0
18	139.4	3.08	24.44	87.0
19	20.5	4.63	23.33	87.0

Table 5g : Meteorological Data for Eight Selected Days

Date: 14/9/1964

Time (h)	Solar Rad. on Hor. Surf (W/m^2)	Wind Speed (m/s)	Temp. (^oC)	Rel. Humid (%)
6	0.0	2.06	15.56	93.0
7	41.9	2.06	15.00	93.0
8	260.2	2.06	15.00	84.0
9	482.5	3.08	17.22	78.0
10	671.4	3.08	20.00	70.0
11	809.2	2.06	22.78	71.0
12	884.5	1.54	23.89	68.0
13	757.4	1.54	25.00	60.0
14	828.5	3.08	25.56	56.0
15	407.0	3.08	25.00	52.0
16	432.7	2.57	26.11	52.0
17	182.2	2.57	26.11	52.0
18	64.8	2.57	26.11	55.0
19	0.0	1.54	24.44	68.0

Table 5h : Meteorological Data for Eight Selected Days

Date: 1/10/1964

Time (h)	Solar Rad. on Hor. Surf (W/m^2)	Wind Speed (m/s)	Temp. (^oC)	Rel. Humid (%)
6	0.0	2.60	16.67	97.0
7	4.0	3.60	16.67	97.0
8	107.6	3.60	16.67	100.0
9	118.7	4.11	16.67	97.0
10	306.3	4.63	17.22	100.0
11	348.6	4.11	17.78	97.0
12	611.8	3.60	18.33	97.0
13	380.1	3.60	20.00	97.0
14	559.7	5.14	20.00	97.0
15	168.1	5.65	20.56	93.0
16	214.0	5.14	21.11	87.0
17	58.4	4.63	21.11	90.0
18	6.5	4.63	21.11	87.0
19	0.0	5.14	21.11	90.0

BIBLIOGRAPHY

1. L. B. Anderson and H. E. Rauch, "Application of Optimization Techniques to Solar Heating and Cooling", Journal of Energy 1, No. 1, 18 (1977).

2. B. E. Arthur and Y. C. Ho, Applied Optimal Control, John Wiley and Sons, Inc., New York (1975).

3. ASHRAE Handbook of Fundamentals, New York, Am. Soc. Heating Refrigerating and Air Conditioning Engineers (1972).

4. L. W. Butz, "Use of Solar Energy for Residential Heating and Cooling", *M. S. Thesis, University of Wisconsin (1973)*.

5. P. I. Cooper, "The Absorption of Solar Radiation in Solar Stills", Solar Energy 12, 3 (1969).

6. J. A. Duffie and W. A. Beckman, Solar Energy Thermal Processes, John Wiley and Sons, Inc., New York (1974).

7. F. S. Frederick, "Flat-Plate Solar Collector Performance Evaluation with a Solar Simulator as a Basis for Collector Selection and Performance Prediction", Solar Energy 18, 451 (1976).

8. H. C. Hottel and A. Whillier, "Evaluation of Flat-Plate Solar Collector Performance", Proceedings of the Conference on the Use of Solar Energy, University of Arizona, Vol. II, 74 (1958).

9. H. C. Hottel and B. B. Woertz, "The Performance of Flat-Plate Solar Collectors", Trans. ASME 64, 91 (1942).

10. S. A. Hovanessian and L. A. Pipes, Digital Computer Methods in Engineering, McGraw-Hill Book Company, Inc., New York, 214-269 (1969).

11. B. J. Jennings and S. R. Lewis, Air Conditioning and Refrigeration, International Textbook Company, Scraton, Pennsylvania, (1965).

12. S. A. Klein, P. I. Cooper, T. L. Freeman, D. M. Beckman, W. A. Beckman, and J. A. Duffie, "A Method of Simulation of Solar Processes and Its Application", Solar Energy 17, 29 (1975).

13. S. A. Klein, J. A. Duffie, and W. A. Beckman, "Transient Considerations of Flat-Plate Solar Collectors", J. Engineering for Power 96, 109 (1974).

BIBLIOGRAPHY (Continued)

14. M. Kovarik and P. E. Lesse, "Optimal Control of Flow in Low Temperature Solar Heat Collectors", Solar Energy 18, 431 (1976).

15. B. Y. H. Liu and R. C. Jordan, "The Interrelationship and Characteristic Distribution of Direct, Diffuse and Total Solar Radiation", Solar Energy 4, 1 (1960).

16. D. D. McCracken and W. S. Dorn, Numerical Methods and Fortran Programming, John Wiley and Sons, Inc., New York, 311-364 (1964).

17. R. L. Oonk, W. A. Beckman, and J. A. Duffie, "Modeling of the CSU Heating/Cooling System", Solar Energy 17, 21 (1975).

18. I. A. Schack, Industrial Heat Transfer, John Wiley and Sons, Inc., New York, 262-288 (1962).

19. R. W. Southworth and S. L. Deleewv, Digital Computer and Numerical Methods, McGraw-Hill Book Company, Inc., New York, 420-468 (1965).

20. J. F. Van Straaten, Thermal Performance of Buildings, Elsevier Publishing Company, New York (1967).

21. M. Wahlig, E. Binnall, C. Dols, R. Graven, F. Selph, R. Shaw, and M. Simmons, "Control System for Solar Heating and Cooling", Paper Presented at the International Solar Energy Society Meeting, Los Angeles, CA, July 28-August 1 (1975).

22. D. S. Ward, C. C. Smith, and J. C. Ward, "Operational Modes of Solar Heating and Cooling Systems", Solar Energy 19, 55 (1977).

23. Z. R. Willard, "Properties of Humid Air at Other than Standard Atmosphere", Symposium on Air-Cooled Heat Exchanges, 7th National Heat Transfer Conference, Cleveland, Ohio, ASME, Aug. 10, 1964, 134 (1964).

24. B. C. Winn and D. Hull, "Temperature Control for Solar Heating and Cooling of Buildings", Advances in the Astronautical Sciences 33, 319 (1975).